

https://dspace.org/

Aerosol Optical Properties in the South Atlantic Ocean

Wilson, Dale

2012-01-17
http://hdl.handle.net/10539/10991

Downloaded from a DSpace repository. https://dspace.org/





University of the Witwatersrand

School of Geography, Archaeology and Environmental Studies

Climatology Research Group

Aerosol Optical Properties in the South Atlantic Ocean

MSc Dissertation

Dale Wilson
0308176X

Supervisor: Professor S.J. Piketh

DECLARATION

I declare that this dissertation is my own unaided work. It is being submitted for the degree of Master of Science in the School of Geography, Archaeology and Environmental Studies at the University of the Witwatersrand, Johannesburg. It has not been submitted previously for any degree or examination in any other university.



_____

(Dale I. Wilson)

8th day of July 2011

ABSTRACT

Atmospheric aerosols have direct and indirect impacts on the earth's radiation budget and the radiative forcing on the climate system. A large uncertainty exists regarding aerosols and the effect they have on the earth's radiation budget and global change. The distribution, concentration and types of aerosols are therefore of great importance regarding global warming and climate change. The purpose of this study is to present the atmospheric aerosol characteristics found over the South Atlantic, Southern Ocean and Antarctic continent as well as identify their origin. The aerosol optical properties over the South Atlantic and Southern Ocean region is analysed during the South African National Antarctic Expedition 2007/2008 (SANAE 47) take over cruise on board the M/V *S.A. Agulhas*. Very low aerosol optical thickness (AOT) values were obtained for the Antarctic Coastal region with a mean AOT_{500nm} of 0.03 and a mean Angstrom exponent of 1.78. The South Atlantic region showed a mean AOT_{500nm} of 0.06 and a mean Angstrom exponent of 0.72. AOT values for the South African coastal region had a mean AOT_{500nm} of 0.07 and a mean Angstrom exponent of 0.76. Data comparisons confirm that the data acquired during the study are consistent with previous research from the study region. Comparisons were made between the dataset and the MODIS satellite aerosol product. A discrepancy was shown to exist between the MODIS aerosol product and the acquired dataset using the Microtops II Sunphotometer. Both MODIS TERRA and AQUA overestimate AOT at 550nm.

Keywords: Aerosols, Angstrom exponent, AERONET, Antarctica, aerosol optical properties, Climate, HYSPLIT, SANAE IV, South Atlantic, Southern Ocean, MODIS.

PREFACE

Atmospheric aerosols influence climate by scattering and absorbing solar radiation and by altering the microphysical properties of clouds (Power, 2003). There is, however, much uncertainty regarding the radiative forcing on the earth system due to aerosol loading. This uncertainty is due to the lack of data particularly over the oceans, regarding global aerosol distributions, concentrations and aerosol types as well as the extent to which anthropogenic aerosol emissions are affecting climate. Studies regarding aerosol optical properties and the distribution of aerosols are of considerable importance to global climate change science. The Maritime Aerosol Network (MAN), a component of the Aerosol Robotics Network (AERONET) was formed with the aim of creating an archive of aerosol optical data from maritime environments using sun photometry. The aerosol data acquired during this study will add to the MAN network while findings for the study region will fill the gap in aerosol optical data for the south Atlantic, southern ocean and SANAE IV base situated in Antarctica.

For this study, the aerosol optical properties over the South Atlantic, Southern Ocean and SANAE IV base were evaluated during the 140th cruise of the M/V *S.A. Agulhas* dating from the 5th December 2007 to the 22nd February 2008. The specific aims of the study include: identifying and analysing the aerosol optical properties found over the South Atlantic, Southern Ocean and SANAE IV base, identifying the spatial and temporal characteristics of aerosols over the South Atlantic, Southern Ocean and Antarctica from the optical properties and backward trajectory analysis and make comparisons between this study and previous AOT studies, AERONET sites from the study area and the MODIS satellite aerosol product.

The dissertation is divided into six chapters. **Chapter one** provides a detailed background of atmospheric aerosols, their impacts on climate and distribution over the South Atlantic and Southern Ocean as well as outline previous maritime aerosol optical research and gives detailed research objectives for the study. **Chapter two** presents the sampling techniques, data analysis methods and data interpretation methods used in the analysis. **Chapter three**

presents the aerosol optical properties for the entire dataset, a latitudinal analysis as well as a geographical analysis of the dataset. **Chapter four** examines the origins of the aerosols found in the study region using backward trajectory analysis. Trajectories are discussed identifying aerosol origins, transport and possible aerosol types. **Chapter five** presents data comparisons made between this study and previous aerosol studies from both maritime and continental regions. Comparisons are given between previous AOT studies, AERONET sites from study area and the MODIS Terra and Aqua satellite aerosol product. **Chapter six** is the final chapter presenting the important findings and conclusions of this study.

Sections of this dissertation have been presented at the South African Society for Atmospheric Sciences Conferences held in South Africa in 2008 and 2009 an IUP seminar held at Heidelberg University, Germany, August 2008, the International Conference on Planetary Boundary Layers and Climate Change, Cape Town, October, 2009 and the International Polar Year Conference, Oslo, Norway, 2010. Sections of this dissertation have been accepted for publication to the *Journal of Atmospheric Research* under the title "Wilson et al. 2010, Aerosol Optical Properties over the South Atlantic and Southern Ocean during the 140th cruise of the M/V *S.A. Agulhas, Journal of Atmospheric Research.*

The author wishes to thank operational and managerial support from the South African National Antarctic Program (SANAP), the Department of Environmental Affairs and Tourism (DEAT), Brett Kuyper and Isabelle Ansorge (UCT Oceanography Department), Roelof Burger, Shaazia Bhailal and other colleagues at the Climatology Research Group. Many thanks must go to Alexander Smirnov (NASA Goddard Space Flight Centre) for his organization of instrumentation and guidance with data analysis in the study. Professor Stuart Piketh as primary supervisor is thanked for his guidance and opportunities provided throughout the duration of this project. The research was supported by NASA's Giovanni, an online data visualization and analysis tool maintained by the Goddard Earth Sciences (GES) Data and Information Services Centre (DISC), a part of the NASA Earth-Sun System Division.

CONTENTS

Declaration……... i

Abstract…… ii

Preface……..... iii

Contents……... v

List of Tables……... vii

List of Figures…….. viii

Abbreviations and Acronyms…….. x

Chapter 1: Overview……. 1

Introduction…….. 1

Literature Review……. 2

Aerosols…….. 2

Aerosol Types and Origins……... 3

Aerosol Particle Sizes……... 5

Aerosol Optical Properties…… 7

Aerosols and Climate Forcing…….. 9

Aerosol Research……..... 12

Maritime Aerosol Studies……..… 14

Air Mass source regions and associated Airstreams.....….... 20

Research Goals…….……...…. 22

Chapter 2: Data and Methodology…… 23

Study Area……. 23

Instrumentation…….. 24

Instrument Calibration……. 25

Data Collection…….. 26

Data Analysis…….…… 28

Quality Control and Cloud Screening……..…… 28

Angström Exponent Uncertainties…….. 31

Datasets and Statistical Analyses……..... 32
Air Mass Trajectory Analysis…… 34
Data Comparisons……...…….. 35

Chapter 3: Results and Discussion……..... 37
Entire Dataset……..… 37
Latitudinal Analysis……..……..… 40
Geographic Analysis ……....…. 44
African Coastal……...…….…….. 45
Offshore……..….. 45
Antarctic Coastal…….…..… 48
SANAE IV Base, Antarctica…….……..….. 50

Chapter 4: Back Trajectory Analysis – Aerosol Origins for the South Atlantic… 52
African Coastal……..…….……. 53
Offshore……..……. 55
Antarctic Coastal……..…… 57
SANAE IV Base……..…… 59

Chapter 5: Data Comparisons……...……..……...… 61
Previous AOT Studies…….. 61
AERONET Comparison..……..... 64
MODIS Comparison……. 66

Chapter 6: Summary and Conclusions…….……..… 69
Aerosol Optical Properties……..… 69
Spatial and Temporal Characteristics…… 71
Comparisons……..…… 72

Annex A……. 74
Annex B……. 75

References……...……...…… 76

LIST OF TABLES

1.1 Aerosol emissions and their relative particle size categories…..…….…… 5
1.2 Aerosol Types and associated optical properties……..… 16
1.3 Summary of previous maritime aerosol studies…….. 17
2.1 Summary of statistical data for different datasets…..…….. 33
3.1 Summary of statistical data for entire datasets…..…….. 37
3.2 Recapitulative table of main results for each region…… 44
3.3 Summary of statistical data for the SANAE IV dataset……... 51

LIST OF FIGURES

1.1 Vertical Profiles associated with aerosol concentrations..……. 6

1.2 Radiative forcing of both natural and anthropogenic aerosols..…… 10

1.3 Measurements made in the NASA SIMBIOS network..…….. 13

1.4 AERONET MAN sites……..…….. 14

1.5: The latitudinal distribution of the aerosol optical depths taken in the Atlantic……..…. 15

1.6 Map indicating air mass source regions…….. 20

1.7 Air masses affecting Southern Africa…….……. 21

2.1 The cruise track for Good Hope IX and X…….……. 23

2.2 The cruise track for Voyage 140……. 24

2.3 Data acquisition in the South Atlantic Ocean…….....… 25

2.4 Data locations for S.A. Agulhas Voyage……. 27

2.5 Flow Diagram used by AERONET's cloud screening algorithm…….. 29

2.6 Box and Whisker Plot of original and screened data…….…….…… 30

2.7 Box and Whisker Plot of original and screened angstrom data…….…… 31

2.8 168 Hour backward trajectory of an air parcel from the SANAE base……...……... 32

2.9 168 Hour backward trajectory of an air parcel from the SANAE base……...……... 33

2.10 AERONET sites used in study……..……. 35

3.1 AOT 500nm overlaid along Ship Track..……..... 38

3.2 K-Means Cluster Analysis on entire dataset……..……. 39

3.3 Latitudinal distribution of AOT across all available wavelengths….……. 41

3.4 Latitudinal distribution of Angstrom exponent and water vapour….……. 42

3.5A NCEP/NCAR Reanalyses of mean surface air temperature……..... 43

3.5B NCEP/NCAR Reanalyses of mean surface specific humidity…….. 43

3.6A Percentage Frequency Histograms of AOT at 500 nm……. 45

3.6B Percentage Frequency Histograms of Angström exponent..... 45

3.7 AOT 500nm versus Angström Exponent Scatter plot for African Coastal Dataset...… 46

3.8A Percentage Frequency Histograms of AOT at 500 nm…….…… 47

3.8B Percentage Frequency Histograms of Angström exponent……..……..…… 47

3.9 AOT 500nm versus Angström Exponent Scatter plot for Offshore dataset…….……..… 48

3.10A Percentage Frequency Histograms of AOT at 500 nm…….……. 49
3.10B Percentage Frequency Histograms of Angström exponent…….…… 49
3.11 AOT 500nm versus Angström Exponent Scatter plot for Antarctic Coastal Dataset.... 50
4.1 NCEP/NCAR Reanalyses of summer wind vectors…….…….…….. 53
4.2 168 hour back trajectories for 5th December 2007…….…….……. 54
4.3 168 hour back trajectory for 18th February 2008…….…… 55
4.4 168 hour back trajectories for 15th January 2008……. 56
4.5 168 hour back trajectories for 16th January 2008……. 57
4.6 168 hour back trajectories for 19th December 2007…….…… 58
4.7 168 hour back trajectories for 8th February 2008…….…… 59
4.8 168 hour back trajectories for 3rd February 2008…….…… 60
5.1 AOT 440nm Comparison…….……...……. 62
5.2 AOT 500nm Comparison…….……...……. 63
5.3 AOT 550nm Comparison…….……...……. 64
5.4 AERONET Comparison…….. 65
5.5 MODIS TERRA 550nm Comparison……..…… 66
5.5 MODIS AQUA 550nm Comparison……..…… 67
5.7 Satellite minus sunphotometer retrievals……..…….. 68

ABBREVIATIONS AND ACRONYMS

AERONET	Aerosol Robotics Network
AOT	Aerosol Optical Thickness
ASL	Above Sea Level
cA	Continental arctic
cAA	Continental Antarctic
cP	Continental polar
cT	Continental tropical
DEAT	Department of Environmental Affairs and Tourism
DISC	Data and Information Services Centre
DMS	Dimethyl Sulphide
GES	Goddard Earth Sciences
GDAS	Global Data Assimilation System
GOCART	Goddard Chemistry Aerosol Radiation and Transport
H_2SO_4	Sulphuric Acid
HYSPLIT	Hybrid Single Particle Lagrangian Integrated Trajectory Model
IPCC	International Panel on Climate Change
IUP	Institut für Umweltphysik
MAN	Maritime Aerosol Network
MODIS	Moderate Resolution Imaging Spectroradiometer
mE	Maritime equatorial
mP	Maritime polar
mT	maritime tropical
M/V	Merchant Vessel
NASA	National Aeronautics and Space Administration
NCAR	National Center for Atmospheric Research
NCEP	National Center for Environmental Prediction
NGSFC	NASA Goddard Space Flight Centre

NOAA	National Oceanic and Atmospheric Administration
NO_χ	Nitrogen oxides (includes NO and NO_2)
PCASP	Passive Cavity Aerosol Spectrometer Probe
RSA	Republic of South Africa
Rms	Root mean square
S.A.	South Africa
SANAE	South African National Antarctic Expedition
SANAP	South African National Antarctic Program
SAWS	South African Weather Service
SIMBIOS	Sensor Inter-Comparison and Merger for Biological and Interdisciplinary Oceanic Studies
SO_2	Sulphur dioxide
UCT	University of Cape Town
VOC	Volatile Organic Compound
α	Angstrom Exponent
µm	Micrometer
W m^{-2}	Watts per square metre
τ_{500nm}	Aerosol optical thickness at 500nm

Chapter 1

Overview

In this chapter a detailed background of atmospheric aerosols, associated impacts on climate and the distributions over the South Atlantic and Southern Ocean are discussed. The chapter outlines previous maritime aerosol optical research and gives detailed research objectives for the study.

Introduction

International collaborative projects such as the Maritime Aerosol Network (MAN), a component of the Aerosol Robotics Network (AERONET), and the NASA Sensor Inter-Comparison and Merger for Biological and Interdisciplinary Oceanic Studies (SIMBIOS) have been operating for a number of years and are aimed at creating an archive of aerosol optical data from terrestrial and maritime environments using sun photometers (Knobelspiesse et al. 2004; Smirnov et al. 2003; Smirnov et al. 2009). Ground-based aerosol optical data has been obtained over the years from two techniques, either narrow field of view radiometers or shadow band radiometers (Porter et al. 2000). The Microtops II sun photometer is an example of a narrow field of view radiometer that is ideal for ship-based sun photometer measurements due to its user-friendliness, portability and relatively inexpensive price (Porter et al. 2000). Sun photometers allow for accurate measurements into aerosol optical depths and column water vapour concentrations that can be used as a basis for creating aerosol characterizations and models (Smirnov et al. 2002a). Studies regarding aerosols and their spatial and temporal distributions are important in understanding connections between aerosols and various forcing mechanisms within the earth's systems.

Atmospheric aerosols have direct and indirect impacts on the earth's radiation budget and the radiative forcing on the climate system (Smirnov et al. 2002b; Forster et al. 2007). Anthropogenic forcing due to fossil fuel combustion influences the types and concentrations of aerosols found in the atmosphere and hence the amount of radiative forcing on the system (Forster et al. 2007). Research on atmospheric aerosol's properties is

crucial to fully ascertain the connections between aerosol's and the earth's radiation budget, their global distributions and the impacts of anthropogenic forcing on these aforementioned connections.

According to the IPCC Report (2007, 1) "the chemical and physical properties of aerosols are needed to estimate and predict direct and indirect climate forcing." This study outlines the aerosol optical properties for the South Atlantic Ocean, Southern Ocean and SANAE IV Base in Antarctica. The research analysed the aerosol optical properties of the South Atlantic and Southern Ocean region during the South African National Antarctic Expedition 2007/2008 (SANAE 47) whilst onboard the M/V *S.A. Agulhas*. The study aims to identify the types of aerosols, the origin of the aerosols using backward trajectory analysis as well as compare the results to satellite retrievals and other global studies on aerosols with the ultimate goal of helping reduce uncertainty in global climate change science.

Literature Review

Aerosols

Aerosols can be defined as solid or liquid particles that are suspended in the air (Peixoto and Oort, 1992; Tyson and Preston-Whyte, 2000; Gadhavi and Jayaraman, 2004). Aerosols play a crucial role in the atmosphere; they affect atmospheric visibility, atmospheric radiation, the formation of cloud particles and atmospheric electricity (Hobbs, 2000). Climate change and anthropogenic forcing during the 21st century is expected to cause increased concentrations of aerosols globally (Jacob et al. 1995).

Aerosol particles in the atmosphere are caused by two processes, direct injection known as primary aerosols and chemical reactions known as secondary aerosols (Peixoto and Oort, 1992; Seinfeld and Pandis, 1998). Direct injection of aerosols is a result of dust, soot, sea salt particles being directly injected into the atmosphere from events such as volcanoes, forest fires and anthropogenic activities as well as other natural processes. Reactions such as the transformation of SO_2 into H_2SO_4 and NO_χ into nitric acids are examples of

secondary aerosol injections (Peixoto and Oort, 1992). Both natural and anthropogenic aerosol emission events have different spatial and temporal characteristics. Aerosols can be broadly classified into a number of types, namely urban/industrial pollution, biomass burning aerosols, dust and oceanic air and include both natural and anthropogenic induced aerosol injection into the atmosphere (Smirnov *et al.* 2003).

According to Howard and Boucher (2000), atmospheric aerosols are removed from the atmosphere through dry deposition (impact with the earth's surface) or by wet deposition (through precipitation). Lifetimes of tropospheric aerosols vary from a few minutes to several weeks (Howard and Boucher, 2000) while stratospheric aerosols could be in suspension for several years due to the stability of the stratosphere (Power, 2003).

Aerosol Types and Origins

The types of aerosols experienced are dependent on the geographical origins of the aerosols. Aerosols from urban or industrial origins are different in molecular composition to aerosols from marine environments. This is true for aerosols from polar, desert and continental environments (Seinfeld and Pandis, 1998). The sources and hence types of aerosols will be discussed in this section.

Urban aerosols are composed of a mixture of emissions from urban areas, namely industrial, transportation and power generation (Seinfeld and Pandis, 1998). These aerosols are characteristic of fossil fuel combustion events in populated areas (Dubovik et al. 2001). Fine and Coarse mode urban aerosol particles differ in composition and in their origins. Coarse mode aerosols originate through mechanical processes and include aerosols such as soil dust, fly ash and tire wear particles for example (Seinfeld and Pandis, 1998). Fine mode aerosols however contain primary aerosols from combustion sources as well as secondary aerosols from chemical reactions. Types of fine mode aerosols from urban environments include sulphates, nitrates, ammonium and secondary organics (Seinfeld and Pandis, 1998). Sulphate and organic aerosols usually amount to more than half of aerosols mass concentrations found in urban areas (Power, 2003).

Marine aerosols are defined as particles over remote oceans where large-scale transport of continental aerosols is not possible (Seinfeld and Pandis, 1998). According to Hobbs (2000), the oceans constitute one of the most important sources of atmospheric aerosols. The marine aerosol is comprised of two main types. The first of these is the primary sea salt aerosol formed from the mechanical disruption of the ocean surface such as ocean spray, bursting bubbles or wind induced wave breaking (O'Dowd et al. 1997; Seinfeld and Pandis, 1998). Primary sea salt aerosols are relatively large in size (> 2 μm) and are characterised as giant particles (Hobbs, 2000). Sea-salt emission into the atmosphere is dependent on wind speed and gustiness (Jacob et al. 1995). The second aerosol type is known as secondary marine aerosols and is composed of mostly non sea-salt sulphates such as Dimethyl Sulphide (DMS) and organic materials formed through gas to particle conversions (O'Dowd et al. 1997).

Continental aerosols are defined as aerosols originating from remote or rural continental areas and are mostly natural in origin. These areas do not include large scale fossil fuel combustion events typical of urban environments. Aerosols identified in these environments include primary aerosols such as dust, pollens and plant wax and secondary aerosols associated with oxidation products (Seinfeld and Pandis, 1998). It is important to note that continental aerosols do have a degree of anthropogenic influence as there are some biomass burning and fossil fuel combustion events in these environments.

Polar aerosols found near the surface in the Arctic and Antarctic regions are very low in concentration. The Arctic region experiences higher AOT values than the Antarctic region due to the long range transport of pollutants into the Arctic Circle (Seinfeld and Pandis, 1998; Power, 2003). Aerosols found in polar environments include, carbonaceous material from mid latitudes, sulphates, sea salt and mineral dust from arid regions (Seinfeld and Pandis, 1998; Power, 2003). Antarctic aerosols consist of sulphates, sea-salt and mineral particles transported from southern hemisphere arid regions (Power, 2003).

Desert aerosols are defined as aerosols having origins over desert environments. Aerosol types are mostly primary aerosols and include dust, soil and crustal particles usually blown

into the atmosphere (Seinfeld and Pandis, 1998). Desert aerosols are also found over marine environments due to their long lifetime in the atmosphere.

Table 1.1. Aerosol emissions and their relative particle size categories, coarse mode particles are defined as > 1 μm, while fine mode particles are defined as < 1μm. (adapted from Seinfeld and Pandis 1998, p102).

SOURCE	PARTICLE SIZE CATEGORY
NATURAL	
Primary	
▪ Soil Dust (mineral salt)	Mainly Coarse
▪ Sea Salt	Coarse
▪ Volcanic Dust	Coarse
▪ Biological Debris	Coarse
Secondary	
▪ Sulphates from biogenic gases	Fine
▪ Sulphates from volcanic SO_2	Fine
▪ Organic matter from biogenic VOC	Fine
▪ Nitrates from NO_x	Fine and coarse
ANTHROPOGENIC	
Primary	
▪ Industrial dust, etc. (except soot)	Fine and Coarse
▪ Soot	Mainly fine
Secondary	
▪ Sulphates from SO_2	Fine
▪ Biomass burning	Fine
▪ Nitrates from NO_x	Mainly coarse
▪ Organics from anthropogenic Volatile Organic Compounds (VOC)	Fine

Aerosol Particle Sizes

Aerosol particles range from approximately 10^{-4}μm - 100μm depending on the aerosol type, source and relative humidity of the associated air mass (Peixoto and Oort, 1992; Hobbs, 1995; O'Dowd et al. 1997). Particles with a mean radius of 0.001 to 0.1μm are known as Aitkin or accumulation mode particles. Particles that are between 0.1 and 1μm

are known as large particles and those between 1 to 10µm are known as giant particles (Peixoto and Oort, 1992; Power, 2003).

Aitkin particles have a relatively short lifetime in the troposphere and are removed quickly through diffusion processes (Power, 2003). Giant particles are larger and heavier and are also removed quickly from the troposphere through gravitational settling. Large aerosols however are too small to be affected by gravitational settling and too large to be affected by diffusion processes. These aerosols therefore have the longest lifespan in the troposphere and form what is known as the Greenfield gap (Power, 2003). Due to their optical properties, aerosols in the Greenfield gap are more likely to attenuate solar radiation and are of great concern to climate change science studies (Power, 2003).

The vertical profile of aerosol concentrations through the atmosphere is therefore not homogenous. Two dominant aerosol layers exist in the atmosphere, the tropospheric layer at the Earth's surface (0 – 3km) and a stratospheric layer higher in the atmosphere (15 – 25km) (Power, 2003). Aerosol concentrations for marine and remote continental air masses as well as background conditions are higher in the troposphere, whereas aerosols from polar air masses are similar in concentration with height (Figure 1.1).

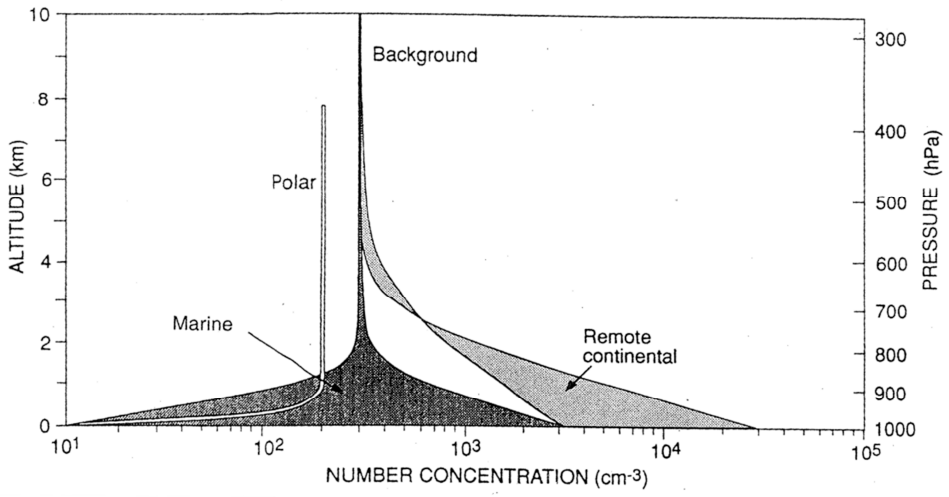

Figure 1.1. The vertical profile associated with aerosol concentrations for marine, polar, remote continental and background air masses (From R. Jaenicke in Hobbs, 2000, p85).

Aerosol size affects the lifetime of aerosols in the atmosphere as well as their physical and chemical properties and impacts on the climate system (Seinfeld and Pandis, 1998, Power, 2003). The optical properties of aerosols are therefore fundamental in the study on aerosols and climate change.

Aerosol Optical Properties

The optical property of an aerosol refers to interaction between light and the aerosol particle. This includes absorption, refraction and reflection of both shortwave and longwave radiation. Aerosol particle size and the complex index of refraction determine the aerosol optical properties (Redemann et al. 2000). Parameters such as aerosol optical thickness (AOT), aerosol size distribution, single scattering albedo, relative phase functions, and the refraction indices describe the optical properties.

According to Power (2003, p506) "Aerosol climatologies are most often expressed in terms of aerosol optical depth". Aerosol optical depth or aerosol optical thickness refers to the total extinction of the solar wavelength entering the atmosphere where a value is given for each recordable wavelength (Masmoudi et al. 2003). The spectral extinction of the direct solar radiation is defined by the Beer-Lambert-Bouguer law:

$$V(\lambda) = V_o(\lambda)(\frac{d_o}{d})^2 e^{(-m\tau_t(\lambda))} \quad (1)$$

Direct solar radiation is measured through filter bands in terms of voltage V and associated wavelength λ. The spectral irradiance signal is a function of the instruments exo-atmospheric voltage V_o, the average distance between the earth and sun d_o, the actual distance between the earth and sun at time of reading d, the solar zenith angle m and the total atmospheric optical depth τ_t (Knobelspiesse et al. 2004).

The relationship between aerosols and their impact on solar radiation was first proposed by Angström in 1929 (King et al. 1978). Angström suggested that the atmospheric aerosol size had an impact on the amount and intensity of radiation at certain wavelengths entering the earth's atmosphere (King et al. 1978). The extinction of radiation from the wavelength due

to the aerosols became known as the extinction coefficient or more commonly known as the Angström exponent (Gobbi et al. 2007). The Angström exponent (α) gives the logarithmic dependence of the AOT on the wavelength in addition to an indirect measure of aerosol size (Queface et al. 2003). According to Masmoudi et al. (2003, 2), "many studies of aerosol optical thickness and its spectral dependence rely on the Angström exponent to quantify this spectral dependence". The optical thickness average spectral dependence, given by the Angström exponent α, can be used to identify the contribution of aerosols to the AOT as well as the size of the aerosols (Gobbi et al. 2007).

The Angström exponent α is calculated by

$$\alpha(\lambda 1, \lambda 2) = \frac{-\ln(\lambda_{\tau 2}/\lambda_{\tau 1})}{\ln(\lambda 2/\lambda 1)} \tag{2}$$

Where λ1 and λ2 refer to known wavelengths and $\lambda_{\tau 1}$ and $\lambda_{\tau 2}$ refers to the associated AOT for the same wavelengths (λ) (Gobbi et al. 2007, 453; Queface et al. 2003). The Angström exponent gives an indirect measure of aerosol particle size and therefore aerosol distribution can be identified. If $\alpha > 1$ then the AOT is defined by fine mode, accumulation mode particles and if $\alpha < 1$ then the AOT is defined by coarse, supermicron particles (Gobbi et al. 2007; Queface et al. 2003).

The flexible inversion algorithm developed by Dubovik and King (2000) identifies a method of deriving the microphysical properties of the aerosols namely, particle size distributions, complex index of refractions and single scattering albedo from sky radiance measurements (Haywood et al. 2003). The methodology outlined by Dubovik and King (2000) has been used frequently in aerosol optical studies with CIMEL Sun photometers (Eck et al. 2005; Haywood et al. 2003; Smirnov et al. 2002a; Smirnov et al. 2002b; Smirnov et al. 2003).

Aerosols and Climate Forcing

Changes in aerosol emissions due to natural and anthropogenic influences have impacts on the earth's radiation budget and is therefore of great concern to scientists. Research on perturbations to this system is required in order to evaluate global and regional climate sensitivity, climate models, predict climate change and clarify the mechanisms of the aerosol radiative forcing (Charlson et al. 2007; Dubovik, 2001). Increased amounts of anthropogenic aerosols in the atmosphere through activities such as fossil fuel combustion and related activities are causing more changes to the system (Charlson et al. 1992).

Perturbations in the radiation budget due to anthropogenic aerosols are equal in magnitude to greenhouse gas forcing, but opposite in sign (Charlson et al. 1992). This suggests that some atmospheric aerosols could offset global warming trends. Urban industrial aerosols, biomass burning aerosols, desert dust and marine aerosols all exhibit different optical properties which affect climate (Dubovik, 2001). Sulphate, fossil fuel organic carbon, fossil fuel black carbon, biomass burning and mineral dust aerosols are examples of aerosols that are emitted into the atmosphere through human induced activities and have a direct influence on the radiative balance (Forster et al. 2007).

Radiative forcing according to Ramaswamy et al. (in Forster et al. 2007, 133) refers to "the change in net (down minus up) irradiance (solar plus longwave; in W m^{-2}) at the tropopause after allowing for stratospheric temperatures to readjust to radiative equilibrium, but with surface and tropospheric temperatures and state held fixed at the unperturbed values". Radiative forcing is thus defined as the change in the balance between incoming solar radiation and the outgoing terrestrial radiation. Radiative forcing at the top of the atmosphere characterises the influence that aerosols have on climate (Keil and Haywood, 2003). Figure 1.2 identifies the global radiative forcing due to various anthropogenic and natural forcing mechanisms. Aerosols have a net negative radiative forcing on the climate system, but the uncertainty surrounding this forcing is high (Forster et al. 2007).

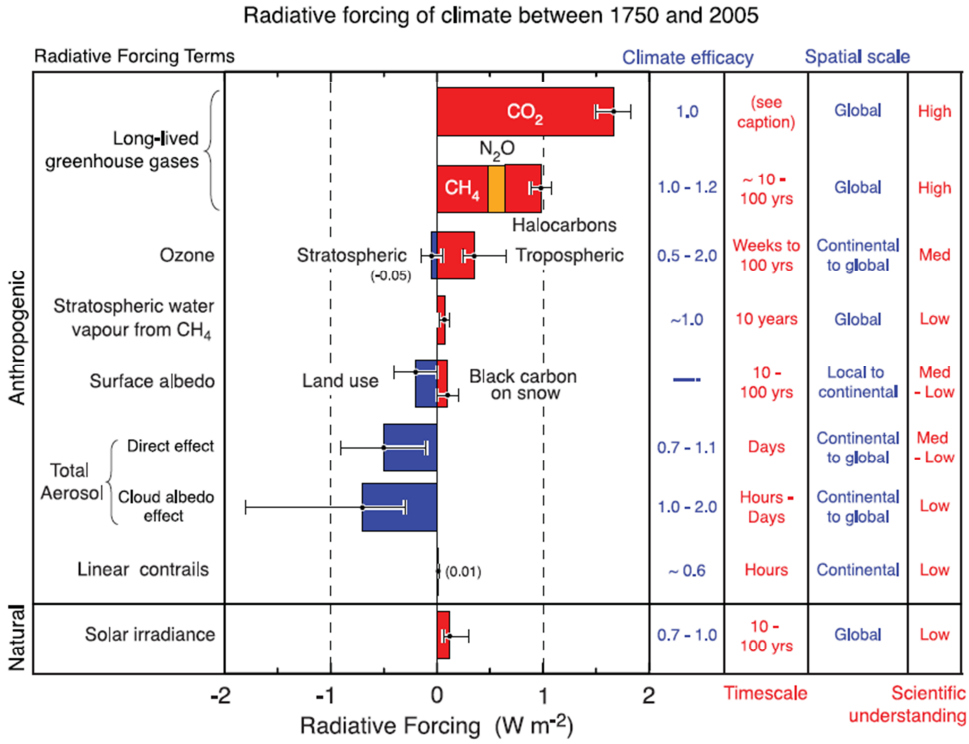

Figure 1.2. The average global radiative forcing of both the anthropogenic and natural forcing mechanisms on the earth system (in Forster et al. 2007, p203).

Aerosol radiative forcing can be categorised into direct and indirect effects both of which have impacts on climate (Forster et al. 2007). Direct effects of aerosols on climate are caused by the scattering and absorption of both shortwave and longwave radiation by aerosol particles, resulting in a change in the radiation balance of the earth atmosphere system (Forster et al. 2007). Some tropospheric aerosols have a cooling influence on climate due to scattering of shortwave radiation and an increase in planetary albedo (Charlson et al. 1992). The direct radiative forcing experienced is dependent on the aerosol optical properties; single scattering albedo, specific extinction coefficient and the scattering phase function which are dependent on wavelength, relative humidity, atmospheric loading and spatial distribution (Forster et al. 2007; IPCC Report, 2007).

Aerosols predominantly affect incoming solar radiation (shortwave), direct radiative forcing is therefore at a maximum during daylight and during summer. Greenhouse gases

however affect both longwave and shortwave radiation, having climate influences during both day and night and throughout the year (Power, 2003). Solomon et al. (2007) suggests that across all aerosols types there is a direct radiative forcing of -0.5 ± 0.4 $W.m^{-2}$ with a medium-low level of scientific understanding. According to Power (2003), aerosols can both increase or decrease planetary albedo resulting in either a cooling or warming effect on climate. The impact on planetary albedo is dependent on aerosol composition, concentration, size, shape and particle albedo (Power, 2003).

Indirect aerosol forcing refers to "the mechanism by which aerosols modify the microphysical and hence radiative properties, amount and lifetime of clouds" (Forster et al. 2007, 153). Indirect forcing is dependent on the effectiveness of the aerosol to form cloud nuclei and is therefore dependant on the aerosol particle size, chemical composition, mixing state and the surrounding environment (Forster et al. 2007). Forster et al. (2007) indicate that there are two effects caused by indirect forcing; cloud albedo effect and the cloud lifetime effect. The cloud albedo effect refers to the effect on droplet number concentrations and size and therefore the ability of the cloud to absorb and scatter radiation. The cloud lifetime effect refers to the impact on the lifetime of the clouds and therefore the time they spend in the atmosphere. Both effects have impacts on the radiation balance and on climate forcing.

Aerosol Research

The link between the radiative forcing attributes of aerosols to climate change has added to the increased interest in aerosol research. Since the early 1960s, better understandings of aerosol generation, evolution and transport have allowed for the link between climate change and aerosols to be studied (Smirnov et al., 2006). However, the monitoring of atmospheric aerosols is a fundamentally difficult problem largely due to variability in meteorological and climate factors of large scale air masses (Dubovik, 2001; Power, 2003). The following section identifies research techniques and studies regarding aerosols in both maritime and terrestrial environments.

Observations regarding the total aerosol column are taken using either ground-based remote sensors such as sun photometers, from satellites using imaging radiometers and from ground based or aircraft using particulate monitoring instruments such as the Passive Cavity Aerosol Spectrometer Probe (PCASP) (Ichoku et al. 2002; Haywood et al, 2003). Ground based sun photometers enable data acquisition from in situ locations whereas satellite observations cover larger areas are best suited for global monitoring of aerosols (Ichoku et al. 2002; Power, 2003). Sunphotometers and satellite aerosol algorithms express aerosols in the atmospheric column in terms of AOT whereas particulate monitoring instruments give aerosol types and concentrations.

Networks such as the NASA SIMBIOS project and the Aerosol Robotics Network (AERONET) are aimed at creating an archive of aerosol optical thickness and sky radiance data for distribution and integration with satellite data (Dubovik and King, 2000; Smirnov et al. 2003). These networks have acquired data from both maritime and terrestrial environments using handheld sun photometers such as the Microtops II and automated sun photometers such as the CIMEL sun photometer. Figure 1.3 shows the data locations of the SIMBIOS instrument pool taken onboard various research vessels. The figure shows how little aerosol research has been done in the south Atlantic region.

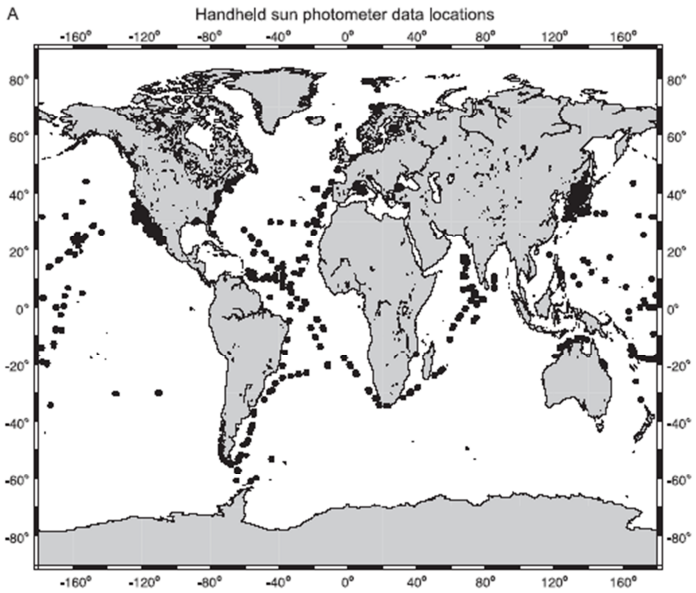

Figure 1.3. Diagram illustrating previous handheld sun photometer measurements from the NASA SIMBIOS network (Knobelspiesse et al. 2004).

Networks such as the Maritime Aerosol Network (MAN), a component of AERONET, was created to collect AOT measurements from the earth's oceans so we may better understand the aerosol optical properties over the oceans (Smirnov et al. 2009). Instruments have been deployed on various research vessels since 2004 (Figure 1.4) monitoring aerosol properties over the world's oceans (AERONET, 2008). The Maritime Aerosol Network allows for a collection of comprehensive aerosol optical depth data from previously unavailable locations. The data made available from the research trip outlined in this study will add to aerosol optical depth database on the Maritime Aerosol Network.

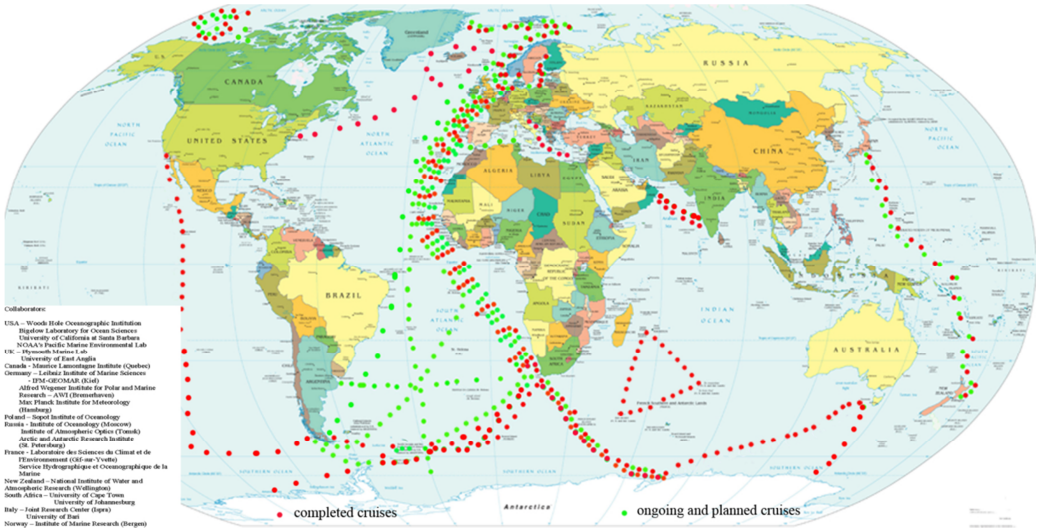

Figure 1.4: AERONET MAN Sites, map identifying cruises on which aerosol optical depth measurements were taken. The Red dots identify completed cruises while the green dots identify ongoing or planned cruises (AERONET, 2008).

Maritime Aerosol Studies

Atmospheric aerosol studies from maritime environments are essential for a comparative study such as the one proposed in this paper. Figures 1.3 and 1.4 identify regions from the world where sun photometer readings have and are being taken. The figures identify a serious lack in the data record regarding the South Atlantic and southern ocean.

A study into Ship-Based Optical Depth Measurements in the Atlantic Ocean (Smirnov et al. 2006) used Microtops II Sunphotometers to identify the AOT in the Atlantic Ocean. The study compared ship-based measurements to satellite retrievals and the GOCART model. The Goddard Chemistry Aerosol Radiation and Transport (GOCART) model simulates global distributions of atmospheric aerosols and aerosol optical depths (Smirnov et al. 2006). The study by Smirnov *et al.* (2006) concluded that atmospheric aerosol optical parameters for the Southern Atlantic correlated well with other oceanic areas (τ_{500nm} ~ 0.04–0.08 and α ~ 0.0–0.4), it was also found that the sun photometer measurements correlated well with satellite retrievals. Figure 1.5 identifies the aerosol optical depth values at 500nm by latitude. The figure gives an idea of the magnitudes of aerosol optical

depths in this region of the world. Attention is drawn to the low AOT values south of -30 degrees south as this coincides with the study region.

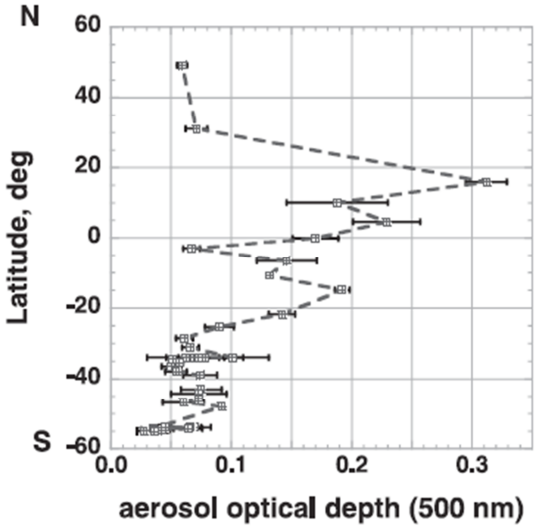

Figure 1.5: The latitudinal distribution of the aerosol optical depths taken in the Atlantic Ocean (Smirnov et al. 2006)

In a study on maritime aerosol optical thickness, Knobelspiesse et al. (2004) classified the entire SIMBIOS AOT dataset into aerosol classification, AOT_{500nm}, Angström exponent and geographic location. Knobelspiesse et al. (2004) found that dust aerosols had the highest AOT_{500nm} at 0.41 followed by continental aerosols at 0.21 and lastly maritime aerosols with a mean AOT of 0.10 (Table 1.2). The study concluded that the maritime data classification compares well with the SeaWiFS aerosol models and automated CIMEL sun photometers from the AERONET network, thus further validating the SIMBIOS dataset. Table 1.2 illustrates the high variability of aerosol extinction properties over oceans, justifying a need for field campaigns in remote oceans to sound aerosol optical properties. Regional classification results from this study are given in Table 1.3. The study by Knobelspiesse et al. (2004) is useful in the classification of aerosols types in terms of their Angstrom and AOT values.

Table 1.2. Aerosol Type and associated AOT 500nm and Angstrom exponent from NASA SIMBIOS data pool (adapted from Knobelspiesse et al. 2004, p100).

Aerosol Classification	AOT 500nm	Angstrom exponent
Dust	0.41	0.58
Maritime	0.10	0.42
Continental	0.21	1.26
Far from Shore	0.18	0.56
Near Shore	0.21	1.12

According to aerosol optical properties, a clean environment is suggested to have an AOT_{500nm} of 0.01 (Porter et al. 2001), background oceanic conditions are suggested to be between 0.06 - 0.08 (Smirnov et al. 2002). AOT values experienced higher than these will have some impact from long range transport of aerosol from urban or continental areas. Eck et al. (2005) describes a highly polluted site in Beijing as having an AOT_{500nm} of 0.7. Smirnov et al. (2002) found that for remote oceanic regions not affected by long range transport of desert dust or volcanic activity had an AOT_{500nm} of below 0.12. Smirnov et al. (2006) found that atmospheric aerosol optical parameters for the Southern Atlantic correlated well with other remote oceanic areas having values of AOT_{500nm} of ~ 0.04 - 0.08 and an angstrom of ~ 0.0 - 0.4, it was also found that the sun photometer measurements correlated well with satellite retrievals. Another study in the South Atlantic between 34°S and 55°S identified AOT_{500nm} of ~ 0.05 and an angstrom of ~ 0.34 (Sakerin et al. 2007). For the Antarctic coastal and Antarctic continent, studies have identified AOT_{500nm} of < 0.05 for areas south of 60°S (Vinoj et al. 2007) and AOT values as low as ~ 0.03 for the Antarctic continent (Gadhavi and Jayaraman, 2004). Aerosol optical properties identified in this study should coincide with previous research from the Antarctic and southern oceans otherwise identifying a significant new source of aerosols for the region.

Table 1.3 summarises previous maritime aerosol studies from various marine environments located around the world. The table gives average AOT values at 400nm, 500nm and 550nm as well as the location of the study and associated air mass.

Table 1.3: Summary of previous maritime aerosol studies giving the optical properties at different wavelengths.

Reference	Air Mass	Region	AOT 440nm	Angström	Comments
Six et al. (2005)	Continental Antarctic	East Antarctica	0.02	1.65	
	Continental Antarctic	East Antarctica - Diamond Dust Events	0.03	1.25	
Reference	**Air Mass**	**Region**	**AOT 550nm**	**Angström**	
Von Hoyningen-Huene and Raabe (1987) in Smirnov et al. (1995)	Continental Tropical	Atlantic Ocean	0.45		
	Maritime Polar	North Sea, Atlantic Ocean	0.07		
	Maritime Tropical	North Sea, Atlantic Ocean	0.13		
Weller and Leiterer (1988) in Smirnov et al. (1995)	Continental Polar	Baltic Sea	0.62		
	Maritime Polar		0.18		
Hoppel et al. (1990) in Smirnov et al. (1995)	Continental Tropical	Atlantic Ocean 30ºN, 70ºW	0.13	1.65	
	Maritime Tropical	Atlantic Ocean 20º-25ºN, 40º-55ºW	0.08	0.95	
	Maritime Tropical	Atlantic Ocean 20º-30ºN, 20º-70ºW	0.13	0.84	
Reddy et al. (1990) in Smirnov et al. (1995)	Continental Polar	Atlantic Ocean 37º-45ºN, 45º-70ºW	0.50	1.15	
	Maritime Polar	Atlantic Ocean 30º-40ºN, 55º-70ºW	0.15	1.00	
	Continental Tropical	Atlantic Ocean 15º-20ºN, 35ºW	0.38	0.37	
Gulyaev et al. (1990) in Smirnov et al. (1995)	Maritime Polar	North Sea, Atlantic Ocean	0.15	0.94	
	Continental Polar	Baltic Sea	0.18	0.90	
		Mediterranean Sea	0.30	0.94	
		Pacific Ocean	0.09	0.97	
	Continental Tropical	Atlantic Ocean	0.30	0.84	
		Mediterranean Sea (1983)	0.22	0.76	
		Mediterranean Sea (1986)	0.19	1.18	
	Maritime Tropical	Pacific Ocean	0.07	0.24	
		Indian Ocean	0.19	0.51	

Table 1.3: Summary of previous maritime aerosol studies giving the AOT at different wavelengths.

Smirnov and Gulyaw (1990) in Smirnov et al. (1995)	Continental Polar	Atlantic Ocean 35º-40ºN, 5º-20ºW	0.14	0.92	
	Continental Tropical		0.20	0.52	
	Maritime Polar		0.13	0.20	
	Maritime Tropical		0.25	0.50	
Von Hoyningen-Huene and Wendisch (1994) in Smirnov et al. (1995)	Continental Polar	Baltic Sea	0.21	1.17	
	Continental Polar		0.20	1.06	
	Continental Tropical		0.29	1.12	
	Continental Tropical		0.24	0.92	
	Maritime Tropical		0.10	0.42	
	Maritime Polar		0.11	0.46	
Eck et al. (2001)	Maritime Equatorial	Kaashidhoo, Maldives (1999)	0.63	0.12	
	Maritime Equatorial	Kaashidhoo, Maldives (2000)	0.51	0.20	
AERONET Site (Level 1.5) Brent Holben (2009)	Continental Antarctic	Marambio 2007 - 2009	0.05	1.79	
AERONET Site (Level 2) Brent Holben (2009)	Maritime Polar	Crozet Island 2005 - 2007	0.05	0.33	
AERONET Site (Level 2) Anatoli Chaikovsky & Philippe Goloub (2009)	Continental Antarctic	Vechernaya Hill 2008 – 2009	0.03	1.27	
Reference	**Air Mass**	**Region**	**AOT 500nm**	**Angström**	
Porter et al. (2001)		Mauna Loa Observatory	0.01		**Very Clean Environment**
Smirnov et al. (2002)	Maritime Tropical	Lanai, Pacific Ocean	0.07	0.76	
	Maritime Tropical	Nauru, Pacific Ocean	0.08	0.43	
	Maritime Equatorial	Tahiti, Pacific Ocean	0.07	0.74	
	Maritime Tropical	Bermuda, Atlantic Ocean	0.14	0.93	
Torres et al. (2002) in Liley and Forgan (2009)		Oceanic Sites	0.05 – 0.15		
		Tropical and Northern Forests	0.05 – 0.20		
		Clean Rural Areas	0.07 – 0.25		

Table 1.3: Summary of previous maritime aerosol studies giving the AOT at different wavelengths.

	Maritime Equatorial	Ascension, Atlantic Ocean	0.13	0.62	
Knobelspiesse et al. (2004)		W North America	0.10	0.94	
		North Atlantic	0.12	0.50	
		Mid Atlantic	0.29	0.22	
		South Atlantic	0.09	0.28	
		Pacific	0.10	0.45	
		South Asia	0.28	1.00	
		East Asia	0.36	1.05	
Eck et al. (2005)		Beijing, China	0.77		
		Dalanzadgad, Mongolia	0.12		
		Mauna Loa Observatory (sea level)	~0.21		
		Lanai, Pacific Ocean	~0.11		
Six et al. (2005) interpolated	Continental Antarctic	East Antarctica	0.02	1.65	
Smirnov et al. (2006)	NA Maritime Polar		0.07	0.41	**Background Oceanic Conditions 0.06–0.08 at 500 nm [Holben et al., 2001; Smirnov et al., 2002])**
	African Dust		0.23	0.35	
	SA Maritime Tropical		0.15	0.61	
	SA Maritime Subtropical		0.08	0.51	
	SA Maritime Polar		0.06	0.38	
Sakerin et al. (2007)	SA Maritime Polar	South Atlantic	~0.05	~0.34	
Vinoj et al. (2007)	SA Maritime Polar	South Atlantic	~0.05		
Gadhavi and Jayaraman (2004)	Continental Antarctic	Antarctica	~0.03		

Air Mass Source Regions and associated Airstreams

An air mass refers to a large volume of air that exhibits uniform properties of temperature and water vapour content influenced by the properties of the air in its source region (Tyson and Preston-Whyte, 2000). Air masses are divided into a number of source regions (Figure 1.6); maritime polar (mP), continental polar (cP), continental arctic (cA), maritime tropical (mT), continental tropical (cT), maritime equatorial (mE) and continental Antarctic (cAA) (Ritter, 2006). The study region outlined in this paper suggests that the continental tropical (cT), maritime polar (mP) and continental Antarctic (cAA) will be important to the study area in this research paper and will be discussed in more detail. The associated air masses affect the source, type, direction and lifetime of aerosols in the atmosphere.

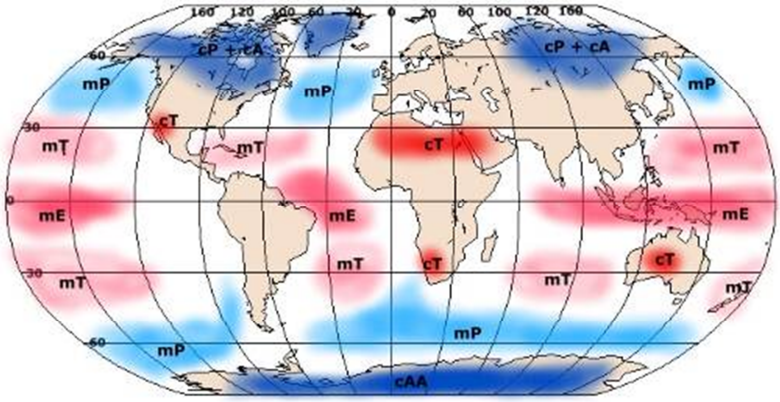

Figure 1.6: The dominant air mass source regions throughout the world. Warmer regions are indicated by the red while bluer regions indicate colder air masses (Ritter, 2006).

The *continental tropical* (cT) air mass is associated with hot and dry conditions of the tropical and subtropical continents (Ritter, 2006). Sources of continental tropical air masses influencing Southern African climate suggest an origin over central Africa as well as desert environments (Tyson and Preston-Whyte, 2000; Ritter, 2006). *Maritime polar* (mP) air mass is associated with cool and moist air responsible for mild weather conditions to coastal locations (Ritter, 2006). The maritime polar air mass and specifically the southerly polar maritime airstream formed off the Antarctic coast results in advection over southern Africa and therefore changes in the mean

temperature (Tyson and Preston-Whyte, 2000). The *Continental Antarctic* (cAA) air mass is associated with extremely cold and dry weather conditions (Ritter, 2006). The continental Antarctic air mass is typically drier than the continental arctic air (cA) of the northern hemisphere due to its origin over the Antarctic continent and lack of precipitation associated with the region (Ritter, 2006).

Airstreams affecting the weather of the African sub continent and South Atlantic Ocean include tropical continental air from central Africa, tropical maritime air from the Indian Ocean and two major cold streams from the South Atlantic and Antarctic coastline (Tyson and Preston-Whyte, 2000). These cold streams are described as a south-westerly sub polar maritime airstream originating in the high latitudes of the South Atlantic and the southerly polar maritime airstream from the Antarctic coastline (Tyson and Preston-Whyte, 2000). Airstreams affecting the chosen study area are identified in Figure 1.7.

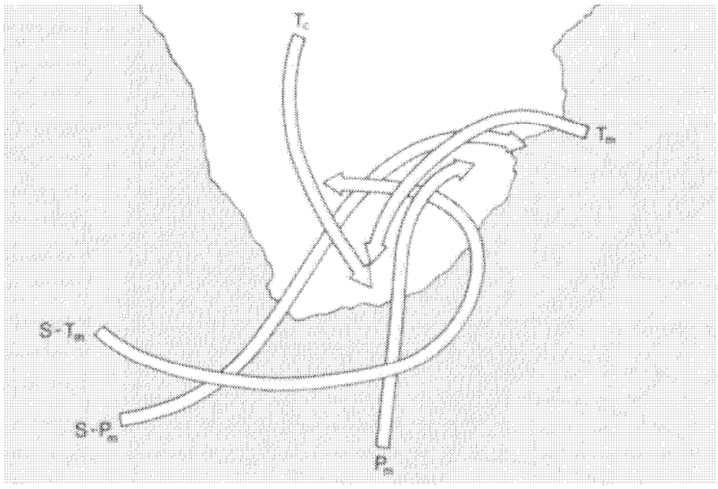

Figure 1.7: Air masses affecting Southern Africa. T_m describes tropical maritime air, T_c describes tropical continental air, $S\text{-}T_m$ describes subtropical maritime air, $S\text{-}P_m$ describes sub polar maritime air and P_m polar maritime air (Tyson and Preston-Whyte, 2000, p135)

Research Goals

The aim of this study is to provide insight into the origin, distribution and optical properties of atmospheric aerosols over the South Atlantic Ocean. This research will add to the global study on atmospheric aerosols and their radiative properties with the goal of reducing uncertainty in aerosol types and distribution and ultimately in global climate change science.

The objectives of the study are:

i. To identify and analyse the aerosol optical properties found over the South Atlantic and Southern Ocean

ii. To identify and analyse first time aerosol optical properties from the South African Antarctic base, SANAE IV

iii. To identify the spatial and temporal characteristics of aerosols over the South Atlantic, Southern Ocean and Antarctica from the optical properties and backward trajectory analysis

iv. To make a comparison between this study and:
    i. Previous AOT studies
    ii. AERONET sites from the study area
    iii. The MODIS satellite aerosol product

Chapter 2

Data and Methodology

Sampling techniques, data analysis methods and data interpretation are discussed in this chapter. Collection of aerosol optical thickness data is defined in terms of the study area, instrumentation and methodology applied. Statistical analyses on the dataset and data comparisons are also discussed.

Study Area

AOT measurements were taken onboard the M/V *S.A. Agulhas* during its 140th Voyage dating from the 5th December 2007 to the 22nd February 2008. The route taken during the voyage followed that of Good Hope IX and X transects (Figure 2.1) outlined by the University of Cape Town's Oceanography department (Swart et al. 2006). The Good Hope transects stipulated a course whereby the vessel departed from Cape Town (33° 55.520'S, 18° 25.428'E) and sailed for the RSA Bukta (ice shelf) in Antarctica. The RSA bukta is located near the South African Antarctic Base known as SANAE IV (71° 40.436' S, 2° 50.311' W; elevation 847m). The timing of the voyage was to coincide with the annual Department of Environmental Affairs and Tourism (DEAT) take-over voyage for the South African National Antarctic Program (SANAP).

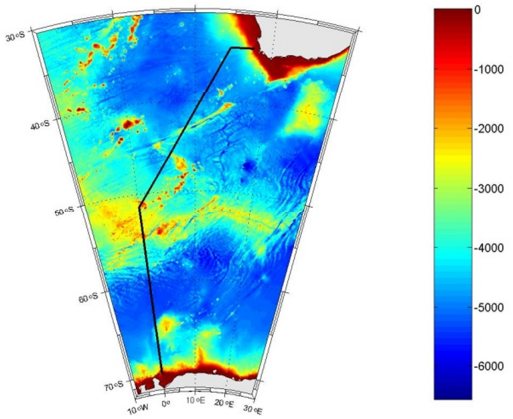

Figure 2.1. The cruise track for Good Hope IX and X, during Voyage 140, overlaid onto the bathymetry of the region (Swart et al. 2006).

Included in the voyage was a Buoy run required by the South African Weather Service (SAWS). The buoy run outlined a cruise track from the RSA Bukta to Southern Thuli (59° 26.458', 27° 18.557' W) and South Georgia Islands (54° 19.408 S, 36° 27.189' W) and then to its most Northern point (49° S, 36° 25.178' W) after which returning back to the RSA Bukta (Figure 2.2).

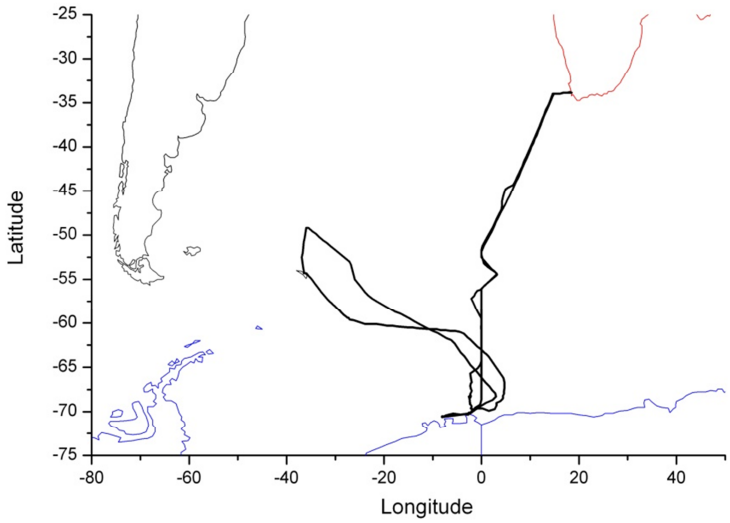

Figure 2.2. The cruise track for *S.A. Agulhas* 140th Voyage. The cruise track includes both the Buoy run and the Good Hope transects.

Instrumentation

Measurements throughout the voyage were taken using a Microtops II handheld sun photometer manufactured by the Solar Light Company (Figure 2.3). The instrument measures direct solar radiation at 5 bandwidths, namely 440, 500, 675, 870 and 936 nm (Morys et al. 2003). The field of view of the Microtops II is 2.5 at full-width half maximum, large enough to allow for sun pointing without significant sunlight into the collimators (Knobelspiesse et al. 2004). The Microtops II Sun Photometer calculates the AOT for each wavelength and the total water vapour in the specific atmospheric column. It is not possible to get all of the aerosol microphysical properties from the Microtops II data.



Figure 2.3. AOT measurements being taken onboard the M/V *S.A. Agulhas* using the Microtops II sun photometer.

Instrument Calibration

Pre and post instrument calibration of the Microtops instruments were performed by the AERONET group at the NASA Goddard Space Flight Centre (NGSFC). A cross calibration technique is used whereby simultaneous measurements are taken using two sun photometers. The one sun photometer is to be used in the field, while the other is a master instrument whose responsivity is well known and documented (Knobelspiesse et al. 2004). A calibration transfer from the master instrument to the field instrument is done so that the field instrument will be accurate once it is deployed. Instrument calibration is important for data accuracy and instrument performance. Pre and post calibration values are needed to assess the accuracy of the instrument and any changes to the instrument performance. According to Ichoku et al (2002) on a study relating to the performance and accuracy of the

Microtops II, it was found that root mean square (rms) differences between calibrated Microtops instruments and the AERONET Cimel master sun photometer were ±0.02 at 340nm decreasing to ±0.01 at 870nm. Ichoku et al. (2002, pg 1) go further to state that the rms differences make the sun photometer "quite accurate and stable" as long as handling errors and inaccurate calibrations are avoided. Other comprehensive studies relating to the performance of the Microtops II have been done by Morys et al. (2001); Porter et al. (2001) and Knobelspiesse et al. (2004). It is important to note that pre-instrument calibration was done by the AERONET group at the NASA Goddard Space Flight Centre. Post-instrument calibration was done by the same AERONET group once the instruments had been shipped back to the Goddard Space Flight Centre.

Data Collection

The Microtops II sun photometer performs several systematic successive measurements within a user defined time (Morys et al. 2003). The Microtops II instrument was set to take triplet (3) systematic measurements within a 10 second period. The averages and standard deviations for each triplet were calculated and one averaged value was stored on the instrument. This method was chosen to accommodate errors that may arise due to movement of the ship and/or impact due to cloud contamination. Together with the systematic measurements it was decided that three separate measurements were to be taken every thirty minutes when the sun was not obstructed by clouds and when the solar zenith angle was not too large. These were chosen to accommodate for any handling errors or interference from clouds. Clouds severely impact the amount of solar radiation entering the sun photometer collimators and therefore the recorded AOT values. In order to acquire as much data as possible, one photometer was sent on the Buoy run and another was sent to the SANAE IV base in Antarctica. Both regions have had little research done on aerosols optical properties.

Data accumulation was largely dependent on weather conditions and available sunlight. With this in mind, the best season in which to perform the study was over the southern hemisphere summer period (December – February) due to the fact that the region below 60°- 63° S is inaccessible due to sea ice for the remainder of the year. The summer period

also offers almost 24 hours of sunlight. The only obstruction in the collection of the data was unfavourable weather and periods during the day when the solar zenith angle was too large. A large solar zenith angle indicates a period when the sun was low on the horizon and would cause the sun to appear dim due to the increased thickness of the atmosphere on the horizon and thus affects the data entry (Solar Light Company, 2003). A Garmin GPS Map 650CSx was used in conjunction with the Microtops II Sun Photometer in order to obtain accurate location parameters and altitude information for each data entry. Daily sun photometer data was stored on the internal memory in the instrument and later downloaded onto a computer using the Microtops II Organizer™ software. A total of eight hundred and fourteen (814) triplet AOT measurements were taken onboard the M/V *S.A. Agulhas* for a total of 36 days including 5 days at the SANAE IB base. Figure 2.4 identifies regions in the South Atlantic, Southern Ocean and Antarctic continent where readings were taken. Gaps in the cruise track identify areas of unfavourable weather conditions. AOT measurements were taken from numerous locations in the South Atlantic as well as first time AOT measurements from the South African base situated in Antarctica, SANAE IV.

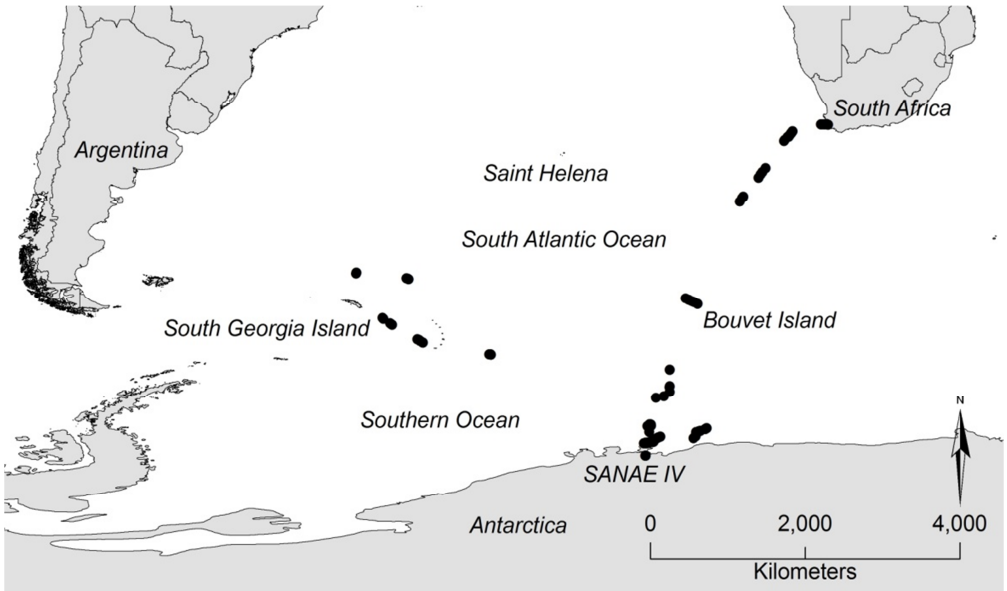

Figure 2.4. Locations in the South Atlantic, Southern Ocean and Antarctic continent where AOT readings were taken using the Microtops II sun photometer.

Data Analysis

Quality Control and Cloud Screening

The separation of cloud affected data from cloud free data is a critical process in AOT studies. Screening these datasets is crucial for the processing and quality assurance of the study (Smirnov et al. 2000). Manual cloud screening can be inconsistent and it is therefore important to have computerized automated cloud screening procedures. The AERONET processing algorithm is applied to the CIMEL and Microtops II sun photometers, instruments within the AERONET MAN network. The AERONET quality control algorithm was applied to the acquired dataset on return to South Africa.

The AERONET quality control algorithm performs data quality checks to ensure that the AOT values obtained from the instrument are not cloud contaminated. Firstly, if the AOT is less than -0.01 for any wavelength, it is excluded from the dataset. Negative AOT values are inaccurate and implausible and can be attributed to cloud interference (Smirnov et al. 2000). Low AOT values can also be attributed to instrument calibration, temperature, atmospheric pressure and column ozone uncertainty (Smirnov et al. 2000). Secondly, if the air mass factor for a specific measurement is greater than 5 then these values are excluded from the dataset. Measurements made at low sun elevations have a higher chance of cloud contamination (Smirnov et al. 2000). The following checks are automatically done by the AERONET algorithm:

- The triplet stability criterion refers to the change in AOT over a one minute period for all wavelengths. The three measurements should not vary by less than 0.02 for the atmosphere to be considered stable and cloud free (Smirnov et al. 2000).

- The diurnal stability check verifies whether the daily standard deviation for AOT at 500nm is less than 0.015.

- The smoothness criterion limits the root mean square of the AOT second derivative with time, a test sensitive to AOT changes due to clouds.

- The three standard deviation criteria checks whether any measurement made by the instrument falls outside the three standard deviation range (3σ) for both the Angstrom parameters and AOT's at 500nm. Smirnov et al. (2000, p346) suggest that "the probability of obtaining a value deviating from the mean of a given sample by more than 3σ is equal to 0.003". All measurements differing by 3σ or more is therefore considered highly improbable and eliminated (Smirnov, 2000).

Figure 2.5 shows the flow diagram describing the cloud screening and quality control algorithm used by AERONET. The Maritime Aerosol Network (MAN) at the NGSFC applied the AERONET quality control algorithm to the Microtops dataset.

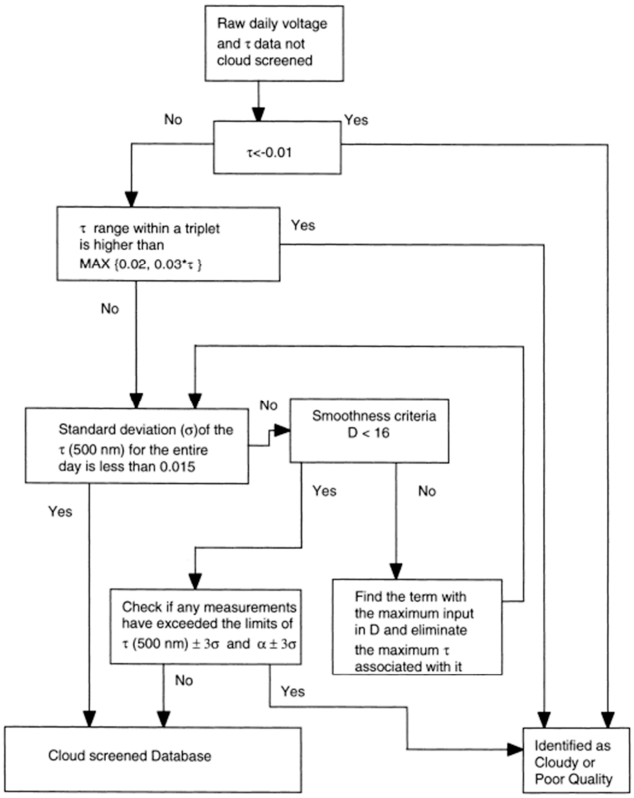

Figure 2.5. The flow diagram used by the AERONET group describing the cloud screening algorithm (from Smirnov et al. 2000, p339).

Statistical analysis of the dataset is required so that final analysis of the dataset is accurate and reflects the true conditions associated with the study area. The minimum, maximum,

mean and standard deviation values were obtained for these values. These values are important to identify variability in both AOT magnitude and Angstrom, essential in quality control of the data. A box and whisker plot of pre and post screened data was created to show differences between the datasets (Figure 2.6). Box and whisker plots are useful in interpreting the distribution of the data and in identifying data points that may affect results.

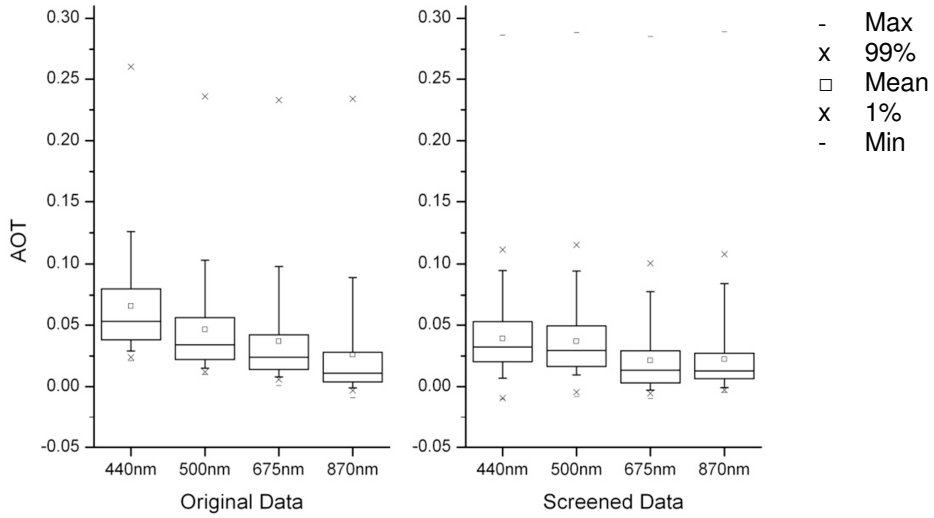

Figure 2.6. Box and Whisker Plot of original dataset taken during the voyage and AERONET screened AOT. Plot shows the max, mean and minimum values as well as the 99% and 1% standard deviations.

Analyses of the box and whisker plots firstly identified that there were AOT outliers below 0 across all available wavelengths. It is not possible to have a negative AOT as this would refer to an aerosol thickness that is less than 0 and nonexistent. Therefore the negative AOT values were removed and excluded from the study. The screened dataset has lower AOT values than the original unscreened dataset.

A least-squares method using all available spectral channels between 440-870nm was used to compute the Angstrom exponent. The box and whisker plot for the Angstrom values (Figure 2.7) showed a number of outliers and a range of positive and negative values. High Angstrom parameters (over 3) are an artefact of low optical depth and a larger uncertainty in Angstrom parameter computations. The AERONET level 2.0

algorithm was applied to the dataset. The level 2.0 algorithm removes unreasonable Angstrom and AOT values from the dataset. These values were further analysed using statistical methods and spatial analyses techniques.

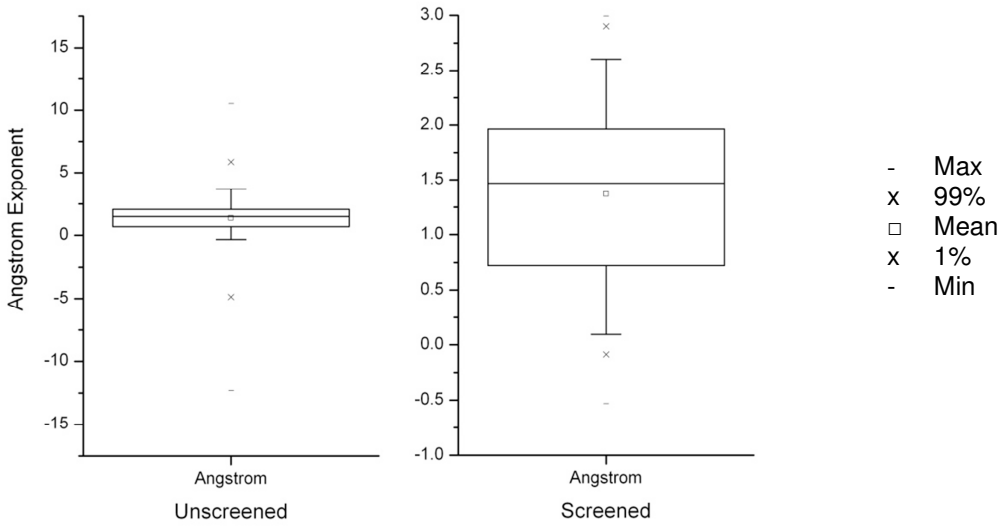

Figure 2.7. The Box and Whisker plots of unscreened and screened Angstrom values for the dataset. The plot shows the max, mean and minimum values as well as the 99% and 1% standard deviations.

Angström Exponent Uncertainties

The use of the Angström exponent as a method of determining aerosol particle size has been well used and documented in aerosol science. Many studies relating to aerosol optical thickness and its spectral dependence rely on the Angström exponent to quantify the spectral dependence (Masmoudi et al. 2003). The Angström exponent further gives and indirect measure of aerosol size. There are however uncertainties relating to the Angström exponent that should be discussed before the data interpretation section of this thesis.

Figure 2.8 shows the Angström exponent versus AOT (500nm) for the entire screened dataset. The graph exhibits very high Angström exponent standard deviations when AOT is low (less than 0.02). A relatively clean environment, such as the one outlined in this study, demonstrating very low AOT values would be accompanied by high uncertainties

associated with the Angström parameter. Coupled with uncertainties and errors associated with the AOT measurements, an AOT (500nm) standard deviation of approximately 0.01 could result in almost 100% error in Angström parameter computations.

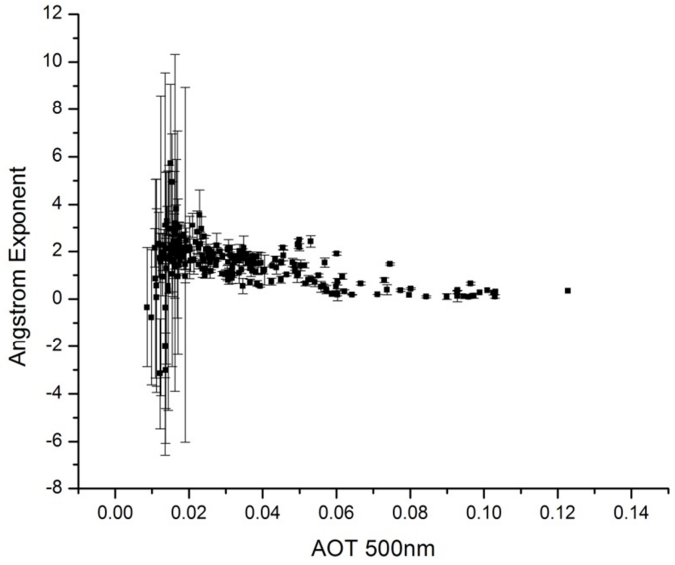

Figure 2.8 The Angström Exponent versus AOT 500nm showing standard deviations for the angstrom exponent.

Despite the uncertainties associated with the computation and error surrounding the Angström exponent, it is still useful to use this parameter as an indirect measure of aerosol particle size. The NASA AERONET processing algorithm is proven to be accurate in removing unreasonable AOT measurements and Angström exponent values (Smirnov et al. 2000). However, the reader of this thesis should be mindful of the high uncertainties surrounding the Angström parameter and deductions made in the thesis.

Datasets and Statistical Analyses

Following the data screening process, the processed data was split into a number of datasets. The first dataset separated the AOT measurements into latitudinal components. This was done to identify the relationship between aerosol optical properties and latitude. AOT and aerosol concentrations are expected to decrease as the distance from continental

sources increases. AOT readings were separated into 5 degree latitudinal averages to identify any latitudinal relationships in the study site.

A second analysis was chosen according to the geographical location of the AOT readings. Following the methodology of Knobelspiesse et al. (2004), those data points situated greater than 300km from a significant landmass where classified as offshore and those closer than 300km were classified as coastal datasets. The use of 300km as a separation point is arbitrary but useful in illustrating the differences between aerosols found close to and far from land (Knobelspiesse et al.). The coastal areas were further divided between Antarctic coastal areas and African coastal areas. This was done to differentiate between continental and marine aerosols. Measurements made at the SANAE IV base were also separated and analysed. The Angström exponent and AOT values allowed for an analyses into the aerosol sizes and their distribution throughout the coastal and offshore data sets. Table 2.1 contains various statistical parameters describing the aerosol data set.

Table 2.1: Summary of statistical data for the entire dataset

Dataset	Mean	Median	Standard Deviation	Skewness	Kurtosis
African Coastal					
AOT 440 nm	0.07	0.07	0.02	0.02	-1.52
AOT 500 nm	0.07	0.08	0.05	0.11	-1.56
AOT 675 nm	0.05	0.05	0.03	0.11	-2.04
AOT 870 nm	0.05	0.05	0.03	0.10	-2.23
Water Vapour	1.60	1.60	0.11	0.09	-1.88
Angström Exponent	0.76	0.63	0.51	0.26	-1.75
Offshore					
AOT 440 nm	0.06	0.06	0.02	0.55	-0.76
AOT 500 nm	0.06	0.06	0.02	0.48	-0.77
AOT 675 nm	0.04	0.04	0.02	0.59	0.66
AOT 870 nm	0.05	0.04	0.03	0.66	-0.73
Water Vapour	0.96	0.68	0.48	0.55	-1.44
Angström Exponent	0.72	0.66	0.47	0.34	-1.18
Antarctic Coastal					
AOT 440 nm	0.03	0.03	0.01	0.74	0.74
AOT 500 nm	0.03	0.02	0.01	0.87	0.04
AOT 675 nm	0.01	0.01	0.01	0.67	-0.21
AOT 870 nm	0.01	0.01	0.01	0.28	0.08
Water Vapour	0.44	0.44	0.10	0.15	-1.25
Angström Exponent	1.78	1.80	1.03	-1.25	8.09

A difference between the mean and median AOT values (computed for a histogram referenced to a linear AOD scale) would identify a dataset that is not normally distributed. Positive skewness and kurtosis would further justify a non-normal distribution, where most outliers are larger than the mean (Knobelspiesse *et al.* 2004). Percentage frequency histograms of AOT and Angstrom exponents and the relative number of peaks and irregularities in the histograms could indicate several aerosol species present in the dataset (Knobelspiesse *et al.* 2004). AOT histograms with similar mean and medians, more than likely indicates a normally distributed dataset with a dominant aerosol type.

Air Mass Trajectory Analysis

Air mass trajectory analysis refers to the study of air masses or particles of air as they move through time and space. These particles can be traced either forward or backward in time along their trajectories. Air mass trajectory analysis is used to assist in identifying the sources and directions of pollutant sources transported over long distances (Cobourn and Hubbard, 1999). Trajectory models such as the Hybrid Single Particle Lagrangian Integrated Trajectory Model (HYSPLIT) are useful in identifying the sources (backward) or directions (forward) of air parcels, aerosols or pollutants. The model applies meteorological data to a chosen point and computes either the forward or backward trajectory of that air parcel for a given time frame. Trajectory analysis allows one to distinguish between continental and maritime air flow and in terms of aerosols, identify the sources of aerosols for a specific region. Figure 2.9 illustrates an example of a seven day backward trajectory of an air mass using the HYSPLIT model. The end of the trajectory is marked with a star. The figure easily shows the origin of the air mass, its movement and change in altitudes.

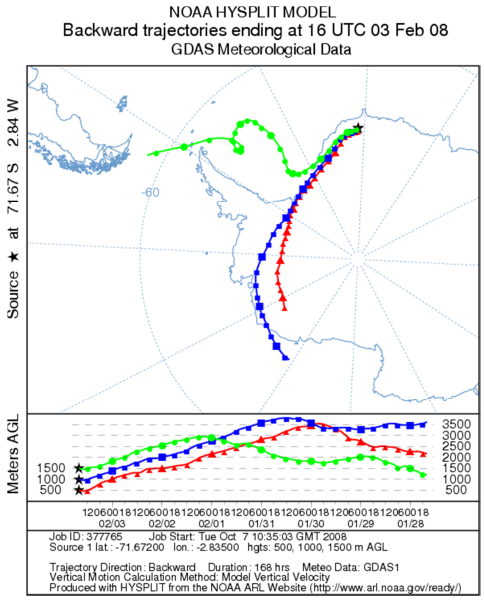

Figure 2.8. An example of a 168 hour backward trajectory of an air parcel from the SANAE IV base situated in Antarctica.

Knowing the source of the air parcel and associated air mass assists in defining what type of aerosol is present in the atmospheric column. Most aerosols have different geographic origins and if these are known, we can infer something about the type of aerosol present. For example, if the backward trajectory analysis identifies that the air parcel originates over a marine environment, we can assume that the aerosols should be of marine origin. It is also important to be familiar with air masses and their source regions. Backward trajectories were run on two locations within each spatial dataset.

Data Comparisons

Data comparisons are essential to evaluate the accuracy of the collected data as well as discrepancies between different instruments. Comparative data is required in order to contextualize the measurements made during the fieldwork. Temporal variations and spatial differences in aerosol properties need to be thoroughly investigated for all datasets. The dataset is compared to previous aerosol studies including both maritime and continental regions. Three AERONET sites (Figure 2.10) situated near the study region are also analysed to compare whether the datasets show similar trends AOT and Angstrom exponents. The AERONET sites chosen as comparisons are identified as

Marambio on the Antarctic Peninsula (64ºS, 56ºW), Crozet Island in the Southern Ocean (46ºS, 51ºE) and Vechernaya Hill situated in Droning Maud Land (67ºS, 46ºE). These sites were chosen as they are the closest AERONET sites to the study area chosen for this project.

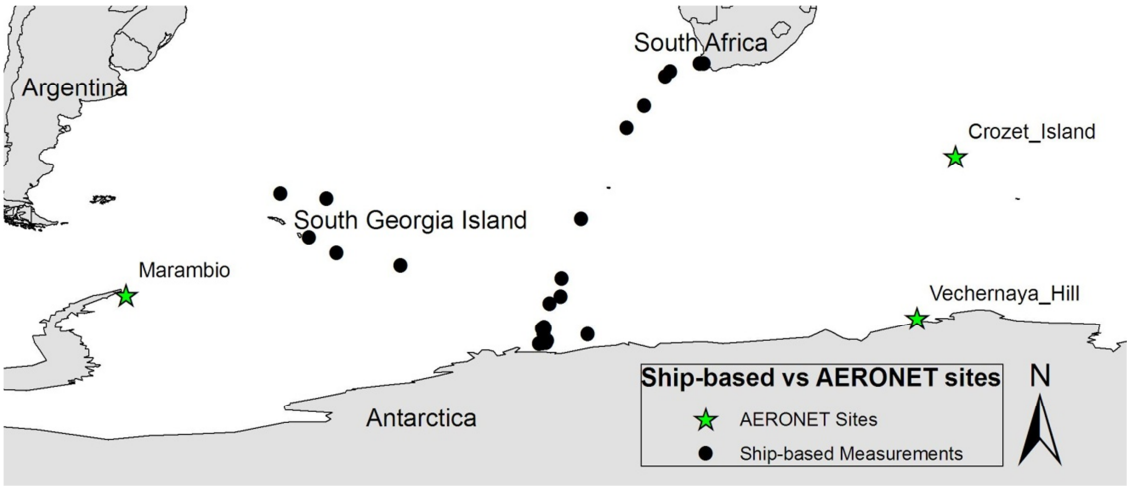

Figure 2.10. The AERONET sites used in the comparison to AOT values for the spatial datasets from the research campaign.

A comparison was done with the MODIS satellite aerosol product to compare differences between ground based and satellite aerosol optical thickness measurements. MODIS MODIS TERRA (version 5) and AQUA (version 5.1) quality assured aerosol product values were compared to Microtops II daily averaged AOT values or matching coordinates and days. The research was supported by NASA's Giovanni, an online data visualization and analysis tool maintained by the Goddard Earth Sciences (GES) Data and Information Services Centre (DISC), a part of the NASA Earth-Sun System Division.

Chapter 3

Results and Discussion

The aerosol optical properties for the study region are presented. Aerosol optical properties are defined for the entire dataset, by latitude as well as by geographical location.

Entire Dataset

AOT measurements taken from the study region suggest aerosols sources to be from maritime, continental and polar environments and therefore the dataset should reflect aerosol types from these environments. An analysis of the entire dataset is done to identify trends in the data and to identify any difference in the geographical areas and the associated aerosols. In a study by Porter et al. (2001), high altitude readings taken at Mauna Loa observatory identify an AOT of $\tau_{500nm} = 0.01$. These high altitude readings at Mauna Loa observatory are indicative of a very clean environment and used in instrument calibration. In comparison, a study by Eck et al. (2005) of Beijing, China, shows an AOT of $\tau_{500nm} = 0.77$, identifying a highly polluted region. AOT values for this study should lie between those clean environments as discussed by Porter et al. (2001) and polluted environments. Measurements taken with the Microtops II sun photometer during the fieldwork campaign identify an AOT daily mean range of $\tau_{500nm} \sim 0.01 – 0.10$ and an Angström exponent range $\alpha \sim 0.12 – 2.36$ for the entire dataset. Table 3.1 identifies statistical parameters describing the data set.

Table 3.1. Statistical values for the entire dataset.

Dataset	Mean	Median	Standard Deviation
All Data			
AOT 440 nm	0.05	0.04	0.02
AOT 500 nm	0.04	0.04	0.02
AOT 675 nm	0.03	0.02	0.02
AOT 870 nm	0.03	0.02	0.02
Water Vapour	0.73	0.56	0.42
Angström Exponent	1.28	1.31	0.69

According to the locations where AOT measurements were taken (Figure 3.1), the data points identify wind-driven maritime and continental dust aerosols in offshore locations and close to continental regions. These aerosols typically have large particle sizes and therefore relatively small Angström exponents (Knobelspiesse et al. 2004). AOT values experienced throughout the journey are low in comparison to urban/continental regions. The average AOT_{500nm} for the entire dataset is 0.04 suggesting low aerosol optical properties indicative of a clean environment. This is as expected due to the remote location of measurements and the distance from major aerosol sources. A number of peaks in AOT exist around the Southern African coastal region and in the South Atlantic Ocean, near the South Sandwich Islands and South Georgia.

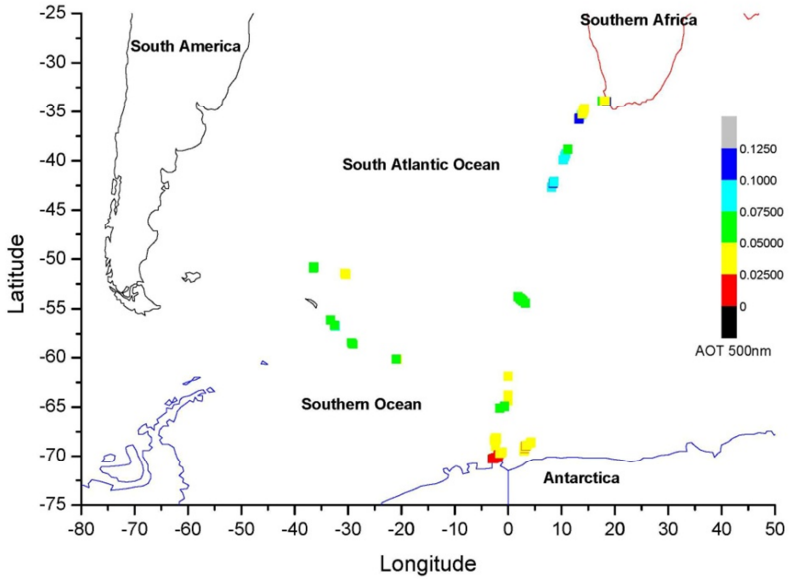

Figure 3.1. The AOT_{500nm} values overlaid along the ship track for the duration of the voyage throughout the South Atlantic Ocean.

The relationship between the AOT and Angström exponent allows one to distinguish between different aerosol species present in the dataset (Knobelspiesse et al. 2004). Clusters indicate the presence of an aerosol type while the location of that cluster on the scatter plot helps identify the aerosol type (Knobelspiesse et al. 2004). Maritime aerosols usually have low aerosol optical thicknesses, usually less than 0.15 and Angström exponents of less than 1.0, (Smirnov et al. 2003; Six et al. 2005). Dust typically has larger

aerosol optical thicknesses associated with larger aerosols, AOT values greater than 0.15 could be attributed to dust particles (Smirnov et al. (2003); Knobelspiesse et al. (2004). The Antarctic environment commonly experiences diamond dust events (ice crystals) (Walden et al. 2003), high Angström values greater than 2.0 could be attributed to these events.

The K-means classification technique for cluster analysis was implemented on the AOT_{500nm} daily means and Angstrom parameter daily mean values (Figure 3.2). Criteria used for the cluster analyses were the minimum Euclidean distance between centroids and object points. Two cluster centres were chosen to reflect a statistical difference between coarse mode and fine mode aerosols found in the study region. Clusters were defined as coarse mode and fine mode aerosols. The separation between the two clusters is roughly just above 1 Angström and consistent with Gobbi et al. (2007) and Queface et al. (2003) regarding aerosol classification. Coarse mode aerosol types include sea salt and dust aerosols while fine mode aerosols include sulphates, nitrates and organic matter. Aerosols in these clusters demonstrate similar optical properties and describe aerosol types from specific locations.

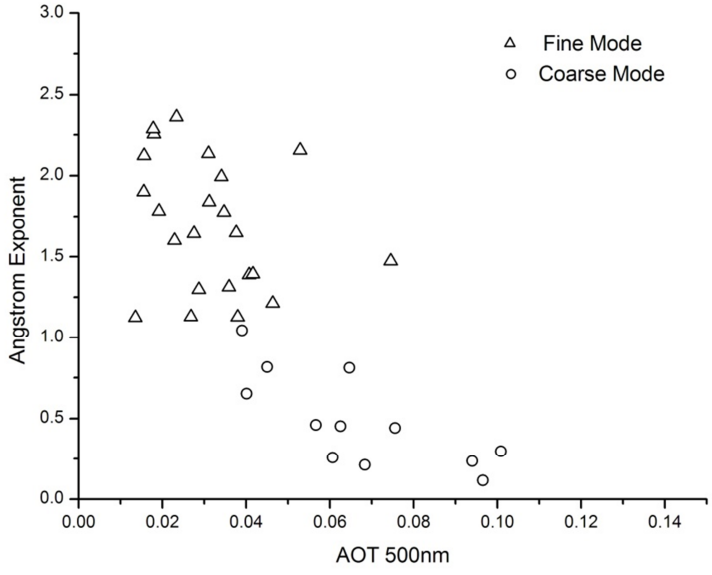

Figure 3.2. K – Means cluster analysis of the AOT_{500nm} daily means and Angstrom parameter daily mean datasets identifying two clusters, coarse mode and fine mode aerosols.

The clustering of the two datasets is a good indication of the quality of the data taken during the voyage while the data range [τ_{500nm} ~ 0.01 – 0.10] is consistent with the study by Smirnov et al. (2003).

Latitudinal Analyses

Smirnov et al. (2009) made a comparison between ship-based AOT measurements taken in the Atlantic Ocean. These cruises were part of the Maritime Aerosol Network (MAN) and include the data taken onboard the M/V *SA Agulhas*. According to the Smirnov et al. (2009) study, an increase in AOT is experienced from 90°N to a maximum AOT over the equatorial Atlantic and then a decrease again to the lowest AOT values over the South Atlantic and Antarctic region. The comparison identified that the AOT values taken onboard the M/V *SA Agulhas* over the 2007-2008 period are consistent with other voyages in the MAN and show very low AOT values for the South Atlantic, Southern Ocean and Antarctic continent.

The AOT trend across all wavelengths (Figure 3.3) shows an increase from Cape Town area to a maximum in the forty degree latitudes. Rough seas and strong winds in this latitude would account for a high sea salt aerosol component being responsible for the high AOT values. Long range transport from continental areas could also be possible. AOT values decrease in the 50 ºS latitudes and increase once again in the 55º S latitudes. From 55º S to 70º S there is a general decrease in AOT across all wavelengths. This could be experienced partly due to the distance from aerosol sources and the occurrence of sea ice absorbing ocean swell and reducing bubble bursting causing sea salt aerosols. Across all wavelengths and latitudes, AOT is below 0.15 describing an unpolluted site.

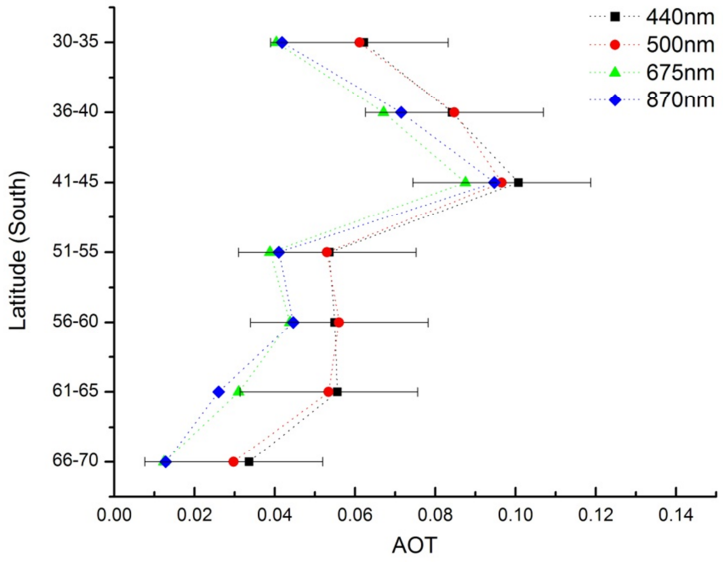

Figure 3.3. The latitudinal distribution of AOT across the four wavelengths measured by the Microtops II sun photometer. Standard deviations are given at the 500nm wavelength.

The distribution of Angstrom exponents by latitude (Figure 3.4) suggests predominantly course mode aerosols until one reaches the extent of the Antarctic summer sea ice at ± 65ºS. At this point, Angstrom values increase and describe the occurrence of predominantly fine mode aerosols. This trend continues further south and describes the aerosol optical properties experienced at SANAE IV base. Water Vapour content by latitude show an almost linear decrease as one approaches the southern polar region.

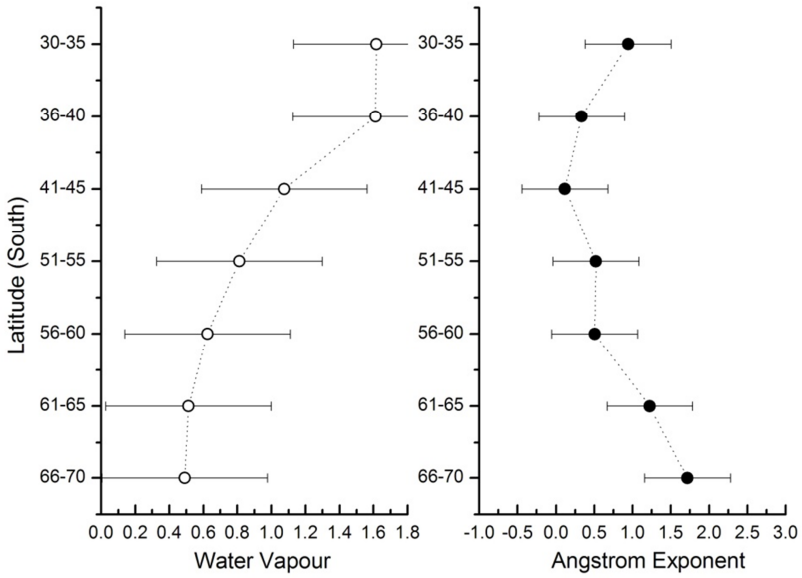

Figure 3.4. Latitudinal distribution of water vapour content and Angstrom exponent including the standard deviations.

A 50 year NCEP/NCAR reanalysis of air temperature and specific humidity identifies a distinct relationship to latitude. Air temperature gradually decreases as one approaches the higher latitudes and Antarctic continent (Figure 3.5a). A decrease in specific humidity is also observed as one approaches the Antarctic continent (Figure 3.5b). An increase in relative humidity is coupled with an increase in aerosol particle size, changes in the aerosol chemical composition and changes in the refractive index (Kay and Box, 2000). Regions experiencing high water vapour concentrations do not necessarily mean small aerosol particles. Large particles are more predominant however total concentration is small and therefore AOT is small. Near Antarctica, smaller particles are experienced due to ice suppressing sea-salt aerosol generation and possible dryer air leading to higher Angstrom parameters.

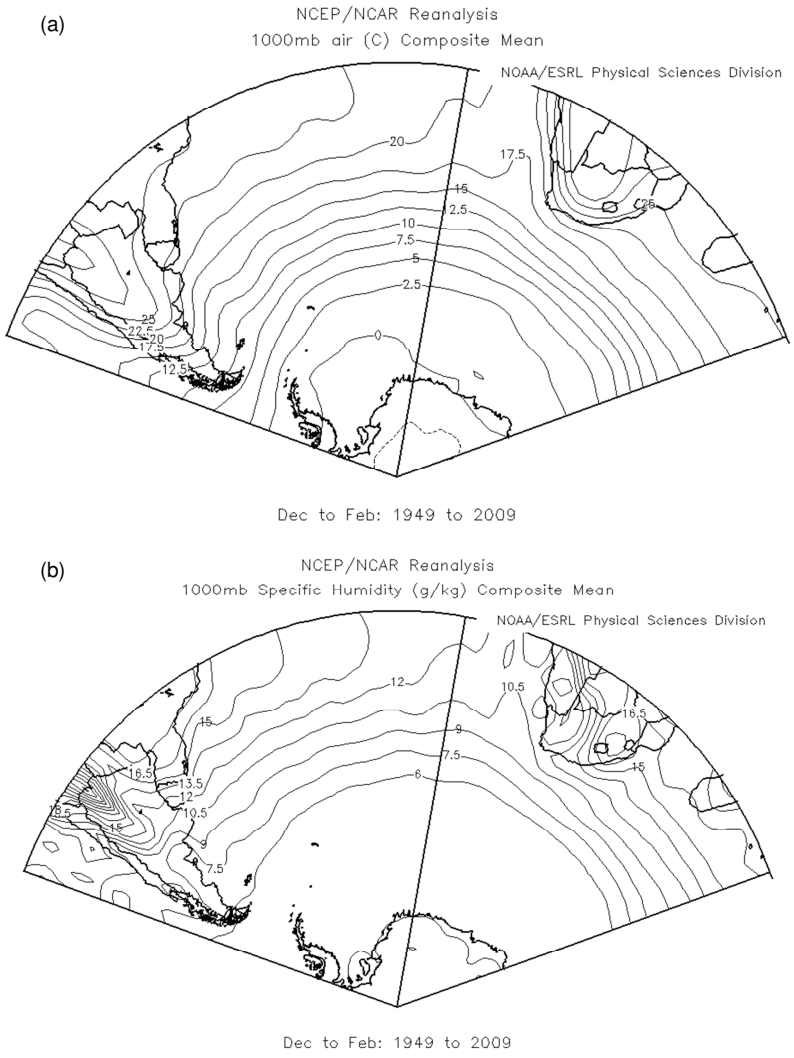

Figure 3.5(a) (b). NCEP/NCAR Reanalysis of (a) composite mean surface air temperature and (b) composite mean surface specific humidity (Kalnay et al., 1996).

Latitudinal comparisons have shown that AOT and water vapour tend to decrease with latitude while Angstrom values increase. There are a number of peaks in AOT at 40º and 55º S. This is due to high wind velocities transporting aerosols and turbulent ocean swells causing sea salt particles. Mostly course mode aerosols are identified until roughly 65º S where the dominant aerosol type is fine mode. This change in aerosol type is experienced together with the occurrence of summer Antarctic sea ice.

Geographic Analysis

The aerosol optical properties were analysed according to geographic location. Following the methodology of Knobelspiesse et al. (2004), those data points situated further than 300km from a significant landmass were classified as offshore and those closer than 300km were classified as coastal datasets. The use of 300km as a separation point is arbitrary but useful in illustrating the differences between aerosols found close to and far from land (Knobelspiesse et al. 2004). Differences in AOT and Angstrom values throughout the voyage can be attributed to the occurrence of different aerosol types. Different aerosol types experienced can be either attributed to direct injection or long range transport of aerosols from other environments. The section will analyse the spatial datasets identifying possible aerosol types.

Table 3.2. A recapitulative table showing mean AOT, Angstrom, standard deviations, skewness and kurtosis.

Dataset	Mean	Median	Standard Deviation	Skewness	Kurtosis
African Coastal					
AOT 440 nm	0.07	0.07	0.02	0.02	-1.52
AOT 500 nm	0.07	0.08	0.05	0.11	-1.56
AOT 675 nm	0.05	0.05	0.03	0.11	-2.04
AOT 870 nm	0.05	0.05	0.03	0.10	-2.23
Water Vapour	1.60	1.60	0.11	0.09	-1.88
Angström Exponent	0.76	0.63	0.51	0.26	-1.75
Offshore					
AOT 440 nm	0.06	0.06	0.02	0.55	-0.76
AOT 500 nm	0.06	0.06	0.02	0.48	-0.77
AOT 675 nm	0.04	0.04	0.02	0.59	0.66
AOT 870 nm	0.05	0.04	0.03	0.66	-0.73
Water Vapour	0.96	0.68	0.48	0.55	-1.44
Angström Exponent	0.72	0.66	0.47	0.34	-1.18
Antarctic Coastal					
AOT 440 nm	0.03	0.03	0.01	0.74	0.74
AOT 500 nm	0.03	0.02	0.01	0.87	0.04
AOT 675 nm	0.01	0.01	0.01	0.67	-0.21
AOT 870 nm	0.01	0.01	0.01	0.28	0.08
Water Vapour	0.44	0.44	0.10	0.15	-1.25
Angström Exponent	1.78	1.80	1.03	-1.25	8.09

African Coastal

The African coastal dataset showed an AOT range of τ_{500nm} ~ 0.03 – 0.12 and an Angström exponent range α ~ 0.12 – 1.53. The dataset has an average AOT_{500nm} of 0.07 and an average Angstrom exponent of 0.76, indicative of a relatively clean environment. Due to the location of data points, AOT's should reflect aerosols from continental/urban and maritime environments. Figures 3.6A and 3.6B identify the percentage frequency histograms for the African coastal dataset. It is important to note that the number of data points used in the African Coastal geographical analyses is small. Only 12 data points were collected from this region as rough seas and cloudy weather affected the Microtops performance. The accuracy of the statistical analyses is therefore of concern, but has been included for the consistency of keeping methodological approaches the same throughout the study.

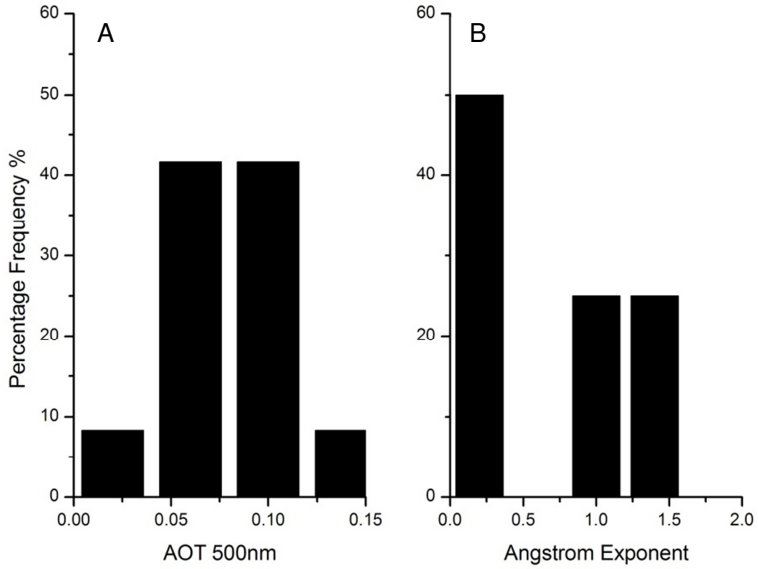

Figure 3.6. Percentage frequency histograms of AOT at 500 nm (A) and Angström exponent (B). Bin sizes used in histogram computation were 0.04 for AOT at 500 nm and 0.4 for Angström exponent.

Figure 3.6A is platykurtic in nature (negative kurtosis) suggesting that the data values are less concentrated around the mean than the corresponding normal distribution. Figure 3.6B is also not normally distributed, strengthening the above mentioned assumption. Mean and median values differ and kurtosis is negative for the

dataset (Table 3.2). The two sharp peaks and irregular nature of the histograms suggests that the dataset is composed of two or more clusters characterizing different aerosol species. This assumption is further strengthened by the AOT 500nm versus Angström exponent scatter plot (Figure 3.7).

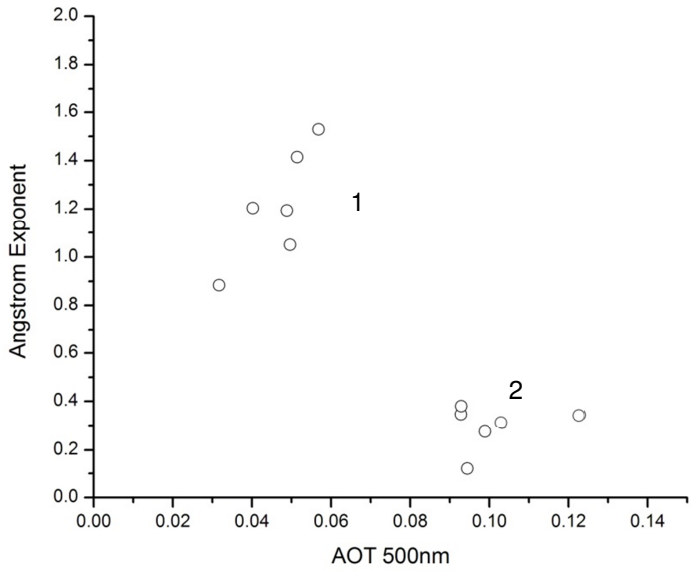

Figure 3.7. AOT 500nm versus Angström exponent scatter plot for the African coastal dataset. Two clusters are shown on the scatter plot.

The scatterplot shows two clusters (labelled 1 and 2, Figure 3.7) which can be attributed to the optical properties of aerosols associated with urban, continental and maritime environments as the locations where these measurements were taken could easily identify all three types of aerosol types. Cluster 1 identifies fine mode, accumulation mode particles as the Angström exponent is greater than 1 while the AOT range is between 0.02 and 0.06. Cluster 1 could be attributed to fine mode aerosols (described in Annexure B). These types of aerosols are located in and around continental regions and include both natural and anthropogenic aerosols. No AOT values were recorded between 0.06 – 0.08.

The distance aerosols travel into the oceans would depend on the aerosol particle size, wind velocity and height in the atmosphere. Cluster 2 identifies coarse mode

particles as the Angstrom exponent is less than 1. Cluster 2 could therefore be attributed to course mode aerosols (described in Annexure B). The origins of these aerosols and further species analyses will be discussed using the backward trajectories of associated air parcels in the following sections.

Offshore

The offshore dataset showed an AOT range of τ_{500nm} ~ 0.03 – 0.10 and an Angström exponent range α ~ 0.09 – 1.61 for the dataset. The dataset shows an average AOT_{500nm} of 0.06 and an average Angstrom exponent of 0.72. The associated AOT values should reflect those aerosols from maritime environments and include sea salt and sulphate aerosols. Figures 3.8A and 3.8B are platykurtic in nature suggesting values are less concentrated around the mean than the corresponding distribution. The negative kurtosis indicates a non normal distribution (Knobelspiesse *et al.* 2004). The non normal distribution of the data and the sharp peaked nature of the histograms suggest more than one aerosol species present in the offshore dataset.

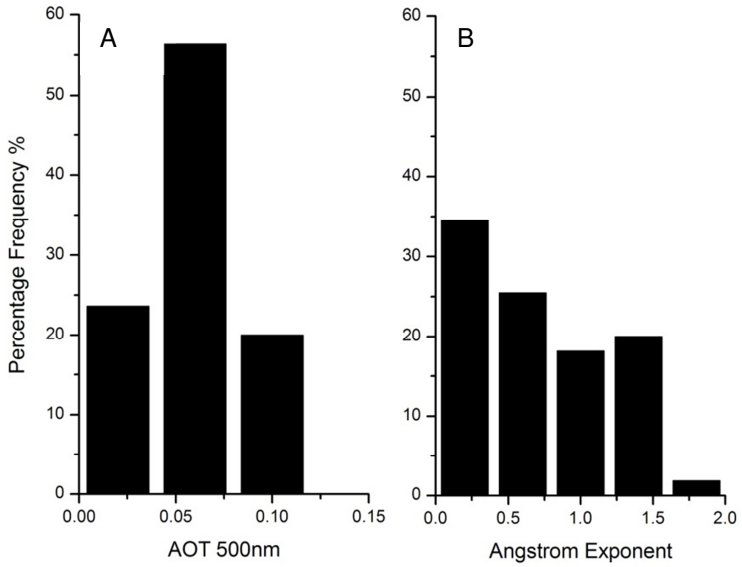

Figure 3.8. Percentage Frequency histograms of AOT at 500 nm (A) and Angström exponent (B). Bin sizes used in histogram computation were 0.04 for AOT at 500 nm and 0.4for Angström exponent.

The dataset showed predominantly course mode aerosols, where 64% of the AOT values had angstrom exponents of less than 1 (Figure 3.9). Due to the location of the dataset, these AOT values associated with low angstrom values would reflect sea salt aerosols as well as a possible influence of long range transport from continental areas suggesting some soil dust and industrial dust affecting the optical properties. Finer aerosols associated with higher angstroms can be attributed to sulphates from biogenic gases such as Dimethyl sulphide (DMS), Organics from VOC's and possible long range transport of fine mode aerosols from continental regions. The optical properties experienced in the dataset describe background oceanic conditions and we would expect backward trajectories to show little contamination from outside sources (Smirnov et al. 2002; Holben et al. 2001).

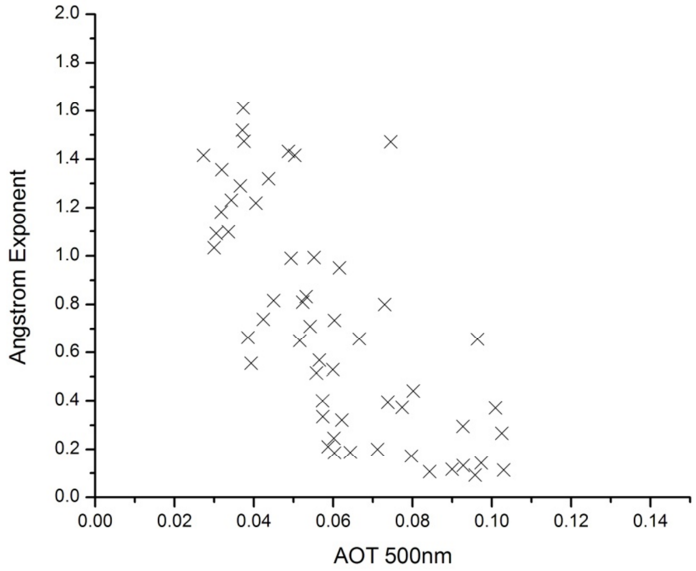

Figure 3.9. AOT 500nm versus Angström exponent scatter plot for the offshore dataset.

Antarctic Coastal

The Antarctic Coastal dataset showed an AOT range of τ_{500nm} ~ 0.01 – 0.06 and an Angström exponent range α ~ 0.08 – 2.30 for the dataset. The dataset showed an average AOT_{500nm} of 0.03 and an average Angstrom exponent of 1.78. The Antarctic region is located very far from industrial and urban aerosol sources. We would therefore expect the aerosols found in the dataset to be from natural emissions, identifying background

conditions from clean polar environments and maritime regions. Low AOT's and high angstrom values identify fine mode aerosols as expected in a clean environment.

The Antarctic coastal percentage frequency histograms (Figure 3.10A and 3.10B) are leptokurtic in nature (positive kurtosis) having a sharper and more acute peak around the mean suggesting a non normal distribution. Similarly to the previous sections, the non normal distribution of the dataset suggests several aerosol species present in the Antarctic coastal dataset but large concentrations of a few aerosols.

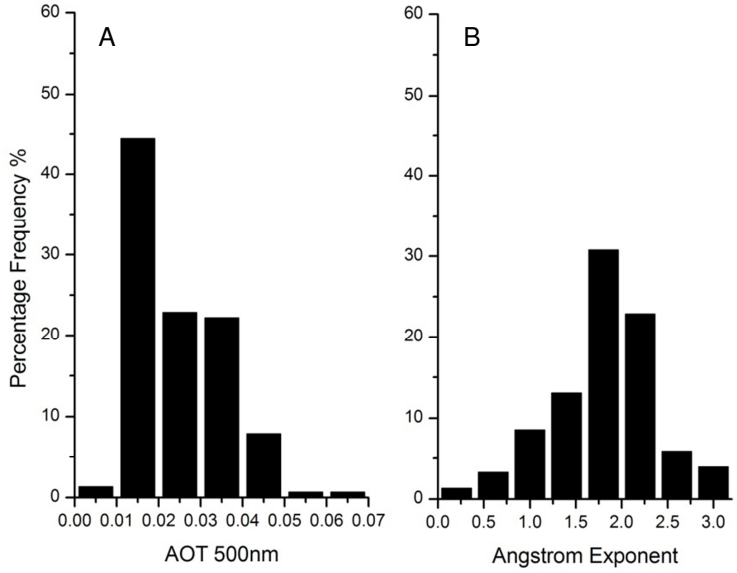

Figure 3.10. Percentage frequency histograms of AOT at 500 nm (A) and Angström exponent (B). Bin sizes used in histogram computation were 0.01 for AOT at 500 nm and 0.4 for Angström exponent.

The comparison of AOT_{500nm} and Angstrom exponent (Figure 3.11) shows that the biggest clustering of optical properties occurs below AOT_{500nm} ~ 0.06 and between 1 and 3 Angstroms. These values define fine mode aerosols namely sulphates, VOC's, nitrates as well as possible diamond dust events (ice crystals) (Six et al., 2005). These aerosols can be found in the Antarctic environment due to long range transport of aerosols, gas to particle conversions as well as direct injection from ships and scientific research bases as well as naturally (ice crystals). Values below 1 Angstrom and between AOT_{500nm} ~ 0 – 0.12 define coarse mode aerosols (Annexure B). These types of aerosols are less

concentrated in the dataset and refer to sea salt particles from maritime environments or larger ice crystals in the atmosphere. Six et al. (2005) found that diamond dust events resulted in higher AOT values. Moisture content and temperatures in the region would affect the size of the nucleation centres for the ice crystals and whether they are fine mode or coarse mode. Backward trajectories will be run on certain points within the dataset to ascertain whether large dust aerosols are possible in the dataset.

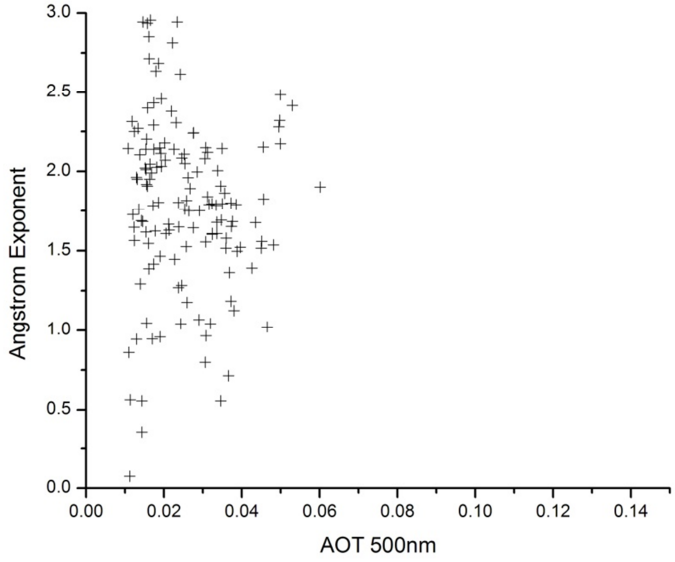

Figure 3.11. AOT 500nm versus Angström exponent scatter plot for the Antarctic coastal dataset.

SANAE IV Base, Antarctica

First time AOT measurements were taken at the South African Antarctic base (SANAE IV) situated in Droning Maud land in Eastern Antarctica (71.7º S, 2.8º W). These data points were screened by the version 1.5 AERONET processing algorithm. The algorithm screens the data for clouds and pointing errors but did not account for calibration errors. High angstrom values excluded from the dataset are an artefact of extremely low AOT values. The small dataset for SANAE IV base and the extremely low AOT values affecting Angstrom exponents do not allow for an analysis into the percentage frequency and thus aerosol types. The low AOT values across all wavelengths suggest a clean environment.

Table 3.3. Summary of statistical data for the SANAE IV dataset

Dataset	Mean	Median	S.D.	Skewness	Kurtosis
SANAE IV					
AOT 500 nm	0.00	0.00	0.02	0.67	-1.77
AOT 675 nm	0.00	0.00	0.02	0.00	-1.59
AOT 870 nm	0.00	0.00	0.00	1.62	4.15
Angstrom Exponent	1.15	1.06	1.21	0.04	-2.09

The dataset (Table 3.3) showed an AOT range of τ_{500nm} ~ 0.00 – 0.04 and an Angström exponent range of α ~ 0.30 – 2.59. Average AOT_{500nm} and Angstrom exponent for the dataset are 0.00 and 1.51 respectively. Low AOT values experienced are similar to those experienced by Porter et al. (2001) at Mauna Loa observatory, suggesting that the SANAE IV base shows evidence of an unpolluted atmospheric column that is relatively aerosol free and indicative of a clean environment. Aerosol species found at the site could be due to long range transport of aerosols from maritime or continental regions or injected into the atmosphere from activities at the base. Similarly to the Antarctic Coastal dataset, we would expect the aerosols type to be composed of mostly fine mode aerosols (Annex B).

Due to the low and sometimes negative AOT values experienced in the 440-870nm range, few Angstrom values could be calculated, not enough to show any trends on a scatter plot. In comparison, Wyputta (1997) states that the main component of aerosols experienced at the Georg-von-Neumayer station is sea salt particles. The Georg-von-Neumayer station is the coastal German Antarctic base and is situated close to SANAE IV. The close proximity of the two bases suggests that they should experience similar meteorological conditions. The dominant sea salt aerosols at the Georg-von-Neumayer station are either transported to other regions, or the aerosols are deposited before they reach SANAE IV.

Chapter 4

Backward Trajectory Analysis – Aerosol origins for the study area

Backward trajectory analyses of air parcels associated with the location of the AOT measurements allows one to trace the origins of the air parcel and therefore possible origins of the aerosols being transported in the air parcel. Backward trajectories were run using the NOAA HYSPLIT model using GDAS meteorological data. Models were run for 168 hours for several locations in each dataset using three heights namely 500m, 1000m and 1500m above sea level and modelled vertical velocity. The following section identifies the backward trajectories for each dataset. These trajectories are discussed identifying aerosol origins, transport and possible aerosol types.

An NCEP/NCAR reanalysis of wind vectors for the months December to February from 1949 to 2008 was run in order to identify a trend in seasonal wind patterns for the study region. The NCEP/NCAR reanalysis derived data was provided by the NOAA/OAR/ESRL PSD, Boulder, Colorado, USA, from their Web site at http://www.cdc.noaa.gov/. The reanalysis derived data (Figure 4.1) identifies an easterly movement of air for the mid latitudes. This movement of air is described by Tyson and Preston-Whyte (2000) as westerly geostrophic flow or the westerlies and describes the regular movement of air throughout the South Atlantic Ocean. Backward trajectories were run using the NOAA HYSPLIT model and should illustrate a similar easterly movement of air through the South Atlantic Ocean.

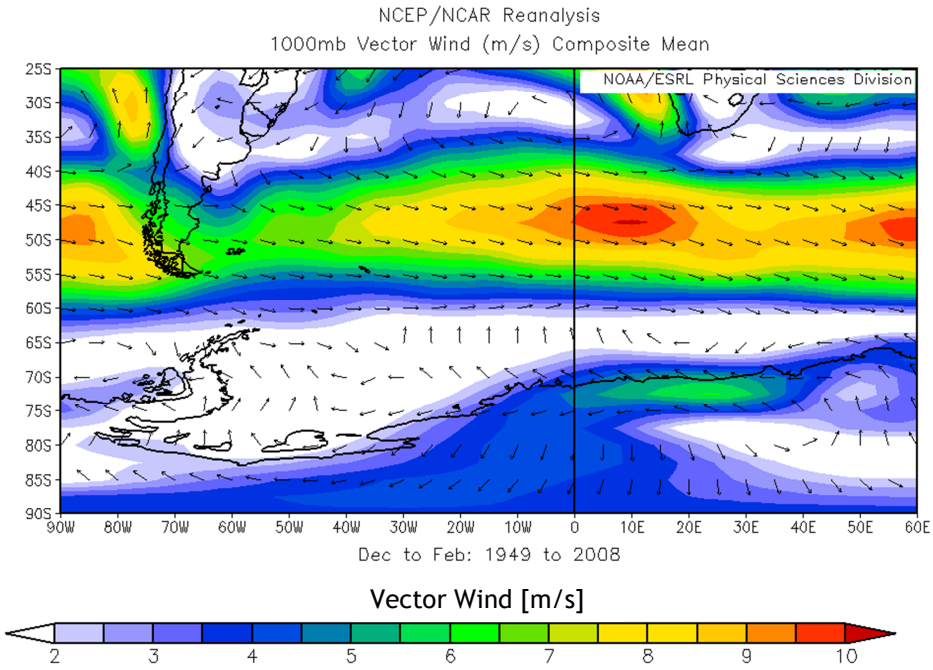

Figure 4.1. The average summer wind vectors for period 1949 – 2008 (Kalnay et al., 1996).

African Coastal

Backward trajectories were run on two locations within the African coastal region. These trajectories coincide with the start and end of the voyage onboard the M/V *S.A. Agulhas*. AOT values for these data points were chosen because they represent different AOT and Angstrom values indicating either course mode or fine mode aerosols. The aim is to identify the origins of the aerosols and make an assumption as to the aerosol type.

The first point chosen was for start of the voyage, the 5th December 2007. A 7 day back trajectory ending on this day was run using HYSPLIT (Figure 4.2). All trajectory heights show a south westerly movement of air from the Antarctic Peninsula and the Drake Passage in the southern ocean. This movement of air is described by Tyson and Preston-Whyte (2000) as westerly geostrophic flow or the westerlies. This movement describes sub polar maritime air from the South Atlantic Ocean and polar maritime air from off the Antarctic coastline. These winds are particularly strong in the in the 40º and 50º southern latitudes and would be a notably strong transport for aerosols from the southern oceans,

Antarctic or South American continent to the Southern African shores. The corresponding data point to the trajectory in 3.12 exhibits an AOT value of $\tau_{500nm} = 0.10$ and an Angstrom exponent of $\alpha = 0.24$. These values suggest course mode aerosols such as soil dust, sea salt, biological debris and Nitrates from NO_x. The back trajectory shows that the air parcel and associated aerosols have origins in the South Atlantic Ocean and should therefore reflect aerosols from this marine environment. We can assume that the coarse aerosols experienced on the 5th of December 2007 were of marine origin and would include sea salts and biological debris.

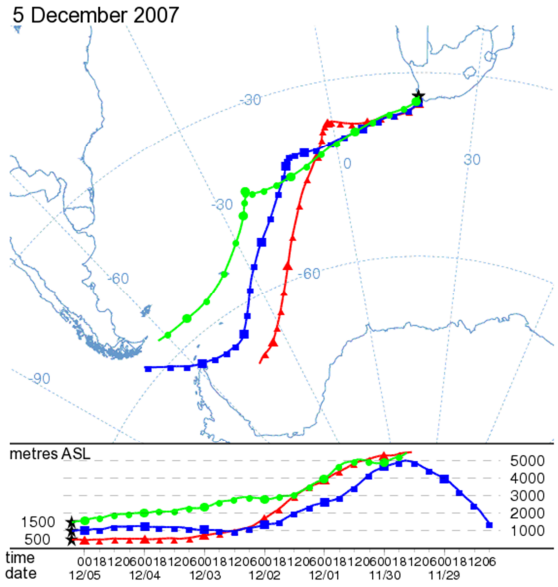

Figure 4.2. The 168 hour back trajectories for 5th December 2007 showing the air parcel to originate in the South Atlantic moving in a westerly direction.

The second point was chosen for the end of the voyage, the 18th February 2008. Backward trajectories were run and show a south westerly movement of air from the Pacific Ocean over Chile and Argentina towards Southern Africa (Figure 4.3). This movement is also described by the westerlies, particularly sub polar maritime air from the south Atlantic. AOT and Angstrom values for the trajectory end point are $\tau_{500nm} = 0.05$ and $\alpha = 1.21$ respectively. The back trajectory suggests that the aerosols experienced on the 18th February 2008 are fine mode and have origins over continental and

marine environments. These aerosols would include fine mode aerosols formed over marine environments such as sulphates from Dimethyl sulphide. Fine mode aerosols originating from continental and urban environments include sulphates from SO_2, nitrates from NO_x and organic matter from VOC's.

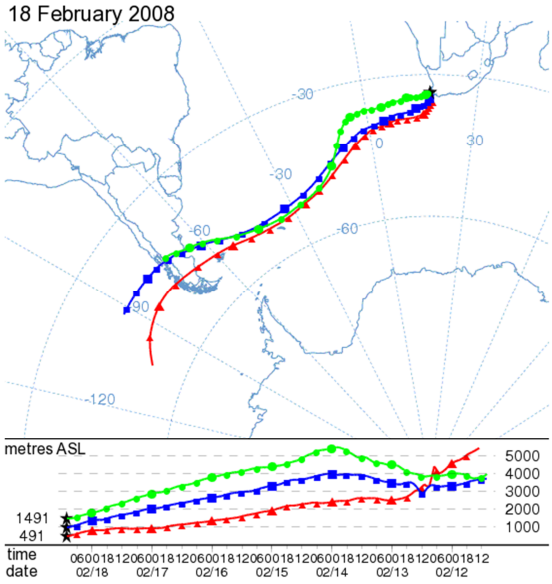

Figure 4.3. The 168 hour back trajectory for the 18th February 2008 showing the air parcel to originate over the South American continent and moving over the South Atlantic ocean in a westerly direction.

Offshore

Similarly to the African coastal dataset, back trajectories were run on two locations within the offshore region. The two data points for which back trajectories were run were from the 15th and 16th January 2008 respectively. These points were chosen because they are temporally and spatially similar but represent large differences between aerosol optical properties.

Backward trajectories were run for 7 days ending on the 15th January 2008 (Figure 4.4). Trajectory heights show that the air parcel at 500m and 1000m (ASL) drops to sea level on the 13th January 2008 and on the 12th January for the higher 1500m trajectory. Aerosols in the air parcel would have been deposited through dry deposition during

impact with the earth's surface. Aerosol species experienced on the 15th January 2008 would therefore have continental origins over South America for the 1500m trajectory and coastal marine origins from the Argentinean coastline for the lower trajectories. Aerosol optical properties for this date show an AOT of $\tau_{500nm} = 0.04$ and an angstrom exponent of $\alpha = 1.04$. These properties describe fine mode aerosols having origins over continental and coastal marine environments. Fine mode aerosols species formed over marine environments include sulphates from Dimethyl Sulphide. Fine mode aerosols originating from continental and urban environments include sulphates from SO_2, nitrates from NO_x and organic matter from VOC's.

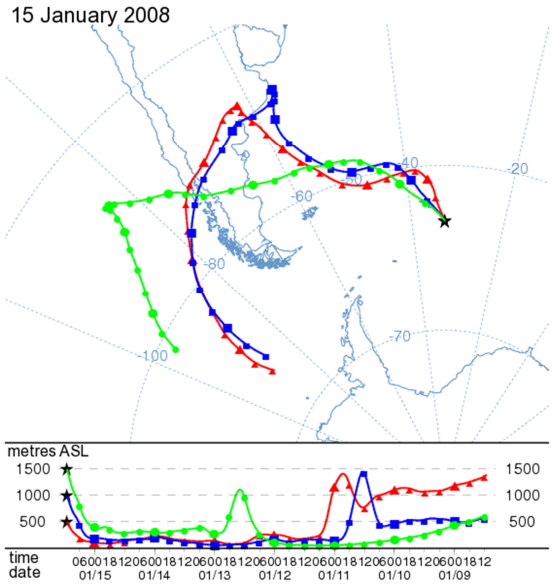

Figure 4.4. The 168 hour back trajectories for the 15th January 2008 showing the air parcel to originate over the Argentinean coastline.

Backward trajectories were run for 7 days ending on the 16th January 2008 (Figure 4.5). Trajectories show the air parcel to originate over the Antarctic continent and then move in a clockwise direction through the Drake Passage toward the South Sandwich Islands. This movement of air is associated with polar maritime air from off the Antarctic coastline as well as continental Antarctic air from the Antarctic continent. Aerosol types experienced would include those from both polar continental regions and marine environments. Aerosol optical properties for this point show an AOT value of

τ_{500nm} = 0.10 and an angstrom exponent of α = 0.16. These values identify coarse mode aerosols having origins over the Antarctic and South Atlantic Ocean. Coarse mode aerosol species originating over the Antarctic landmass and South Atlantic Ocean include sea salt; biological debris; Nitrates from NO_x and ice crystals.

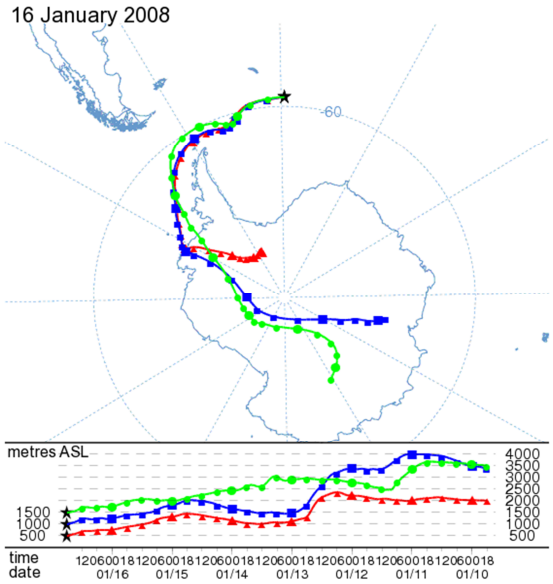

Figure 4.5. The 168 hour back trajectories for the 16th January 2008 showing the air parcel to originate over the Antarctic continent moving in a westerly direction through the Drake Passage.

Antarctic Coastal

Backward trajectories were run on two data points within the Antarctic coastal region. As previously stated, the aerosol optical properties for this region suggest a dataset that is composed of predominantly fine mode particles indicative of a clean environment. The first trajectory identified in Figure 4.6 was run for 19th December 2007. Backward trajectories show the air parcel to have moved in a westerly direction from the east Antarctica coastal region. Aerosol optical properties for this point show an AOT value of τ_{500nm} = 0.04 and an angstrom exponent of α = 1.65. These properties identify fine mode aerosols having origins over continental and coastal marine polar environments. Fine mode aerosols species formed over marine polar environments include sulphates from Dimethyl Sulphide. Fine mode aerosols originating from continental and urban

environments include sulphates from SO_2, nitrates from NO_x and organic matter from VOC's. These aerosols could have been transported to the Antarctic continent from other marine and continental regions where they could have been trapped in the ice only to be re-airborne once the ice melts.

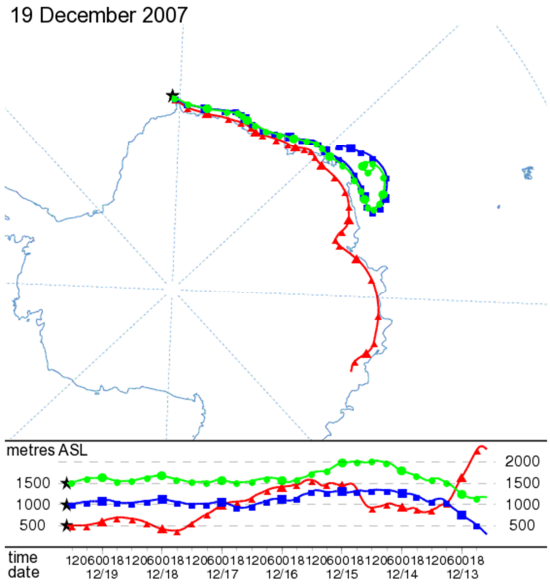

Figure 4.6. The 168 hour back trajectories for the 19th December 2007 showing the air parcel moving in an easterly direction from the Antarctic coastal region.

The second trajectory identified in Figure 4.7 was run for the 8th of February 2008. Backward trajectories show the air parcel to have moved in an easterly direction from the Weddell Sea, past the location of the data point where the air parcel changes direction and moves in a westerly direction back towards the location of the data point. Aerosol optical properties for this point show an AOT value of $\tau_{500nm} = 0.02$ and an Angstrom exponent of $\alpha = 2.40$. Once again aerosol optical properties exhibit a low AOT and high Angstrom exponent indicative of a clean environment and the occurrence of predominantly fine mode aerosols. Similarly to the previous trajectory, fine mode aerosols for this data point should include aerosol species such as sulphates from SO_2 and DMS, nitrates from NO_x and organic matter from VOC's.

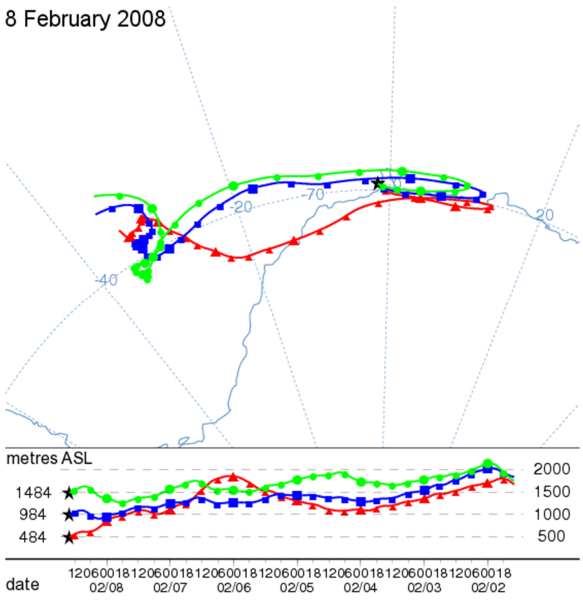

Figure 4.7. The 168 hour back trajectories for the 8th February 2008 showing the air parcel to originate in the Weddell Sea moving in a westerly direction.

SANAE IV Base

A backward trajectory was run on one data point taken at the SANAE IV base. One point was chosen as it reflects the average AOT experienced at the base. As discussed in the previous section, aerosols types experienced are very fine mode and describe a virtually unpolluted site. The backward trajectory was run for 168 hours ending on the 3rd February 2008 (Figure 4.8). The trajectory shows the air parcel to have origins over the Antarctic continent and from over the Weddell Sea for the 500m (ASL) trajectory. If the assumption that sea salt aerosols coming from the nearby Georg-von-Neumayer base are deposited before reaching SANAE IV is correct, then we assume that few sea salt aerosols are experienced at SANAE IV. There are no significant anthropogenic aerosol sources in the Antarctic region other than the maritime component and some base activities. The fine mode aerosols experienced should include aerosol species such as sulphates, nitrates and organic matter from VOC's.

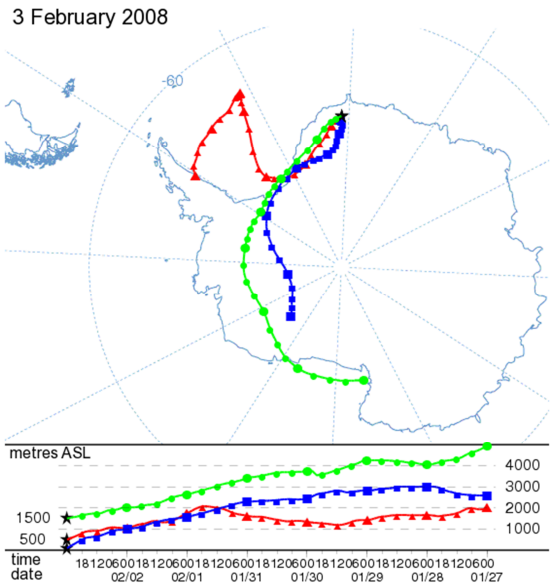

Figure 4.8. The 168 hour back trajectories for the 3rd February 2008 showing the air parcel originating over the Antarctic continent. The lower trajectory run shows the air parcel to originate over the Weddell Sea. All trajectories show a westerly movement the air parcel.

Chapter 5

Data Comparison

Aerosol optical properties from this dataset are compared to previous aerosol studies including both maritime and continental regions. Comparisons are made between three data groups namely previous AOT studies, AERONET sites from study area and the MODIS Terra and Aqua satellite aerosol product.

Previous AOT Studies

Comparisons between this study and from other studies are given. These are made at different wavelengths dependant on the data available from the respective articles. As previously stated, a very clean environment is suggested to have an AOT of $\tau_{500nm} = 0.01$ (Porter et al. 2001), background oceanic conditions are between $\tau_{500nm} = 0.06 - 0.08$ (Smirnov et al. 2002) and a polluted environment can be classed as above $\tau_{500nm} = 0.1$. Comparisons are made at 440nm, 500nm and 550nm and include studies from all over the earth including the South Atlantic Ocean and Antarctic region.

The first comparison (Figure 5.1) is to a study by Six et al. (2005) whereby aerosol optical thickness measurements are given from Dome C in East Antarctica. Six et al. (2005) give two average AOT values, one under normal conditions $\tau_{440nm} = 0.02$ and one under diamond dust events $\tau_{440nm} = 0.03$. Results from this study at 440nm show a higher AOT for the South Atlantic Ocean and South African coastal region and a similar AOT between the Antarctic coastal region and East Antarctica under diamond dust events. The difference between the Antarctic Coastal and East Antarctica AOT is minimal and could be due to the occurrence of marine aerosols in the atmospheric column. The comparison suggests that AOT_{440nm} values are consistent with research done in Antarctica by Six et al. (2005)

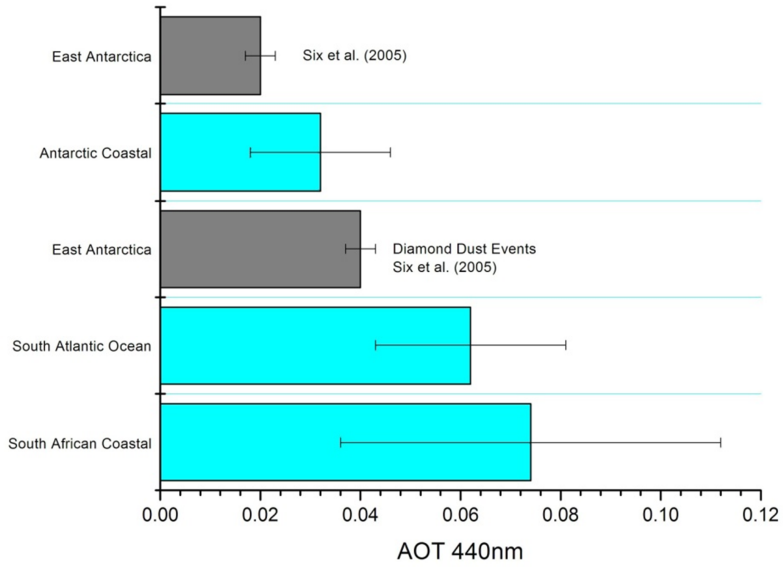

Figure 5.1. AOT 440nm comparison including error bars between this study highlighted in colour and Six et al. (2005) highlighted in grey.

Comparison of AOT_{500nm} to previous studies in the region (Figure 5.2.) shows a large difference between AOT values. The highest AOT value is from Beijing China τ_{500nm} = 0.7, a highly polluted area and the lowest from Mauna Loa Observatory τ_{500nm} = 0.01, a very clean environment. The AOT values for this study are consistent with other studies from marine environments and are situated in relatively clean environments compared to other regions. The AOT values from the South Atlantic are within range for background oceanic conditions as described by Smirnov et al. (2002).

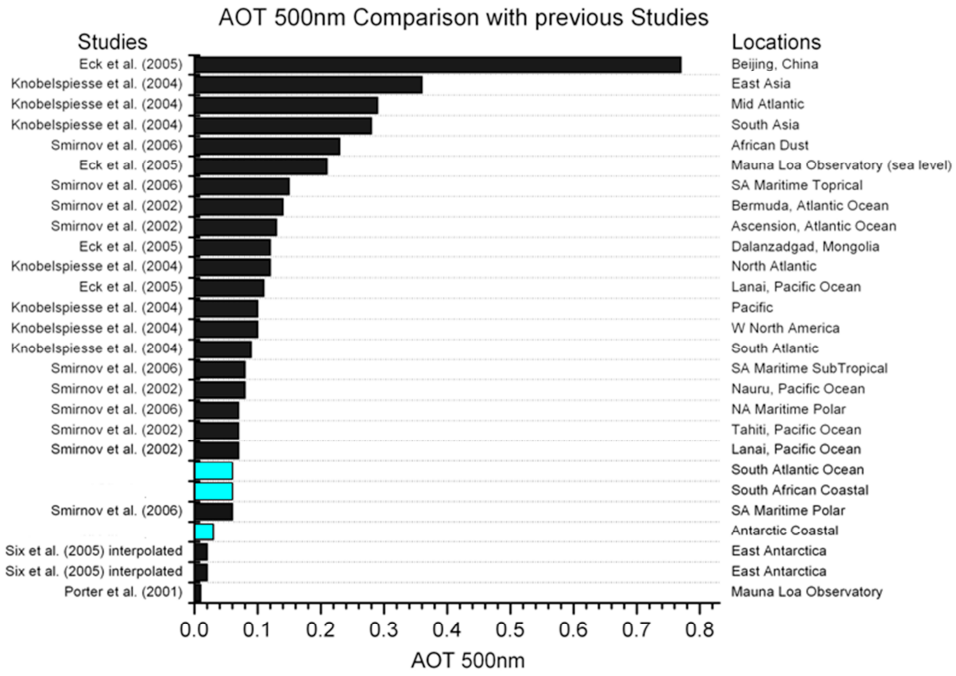

Figure 5.2. An AOT 500nm comparison between this study shown in colour and prior research efforts.

Comparison between AOT550nm for this study and prior research show that values for this study are relatively low compared to other studies (Figure 5.3). These studies are mostly performed in the Northern Hemisphere and in polluted environments; it is therefore understandable that the AOT values for the South Atlantic region and Antarctic region are lower.

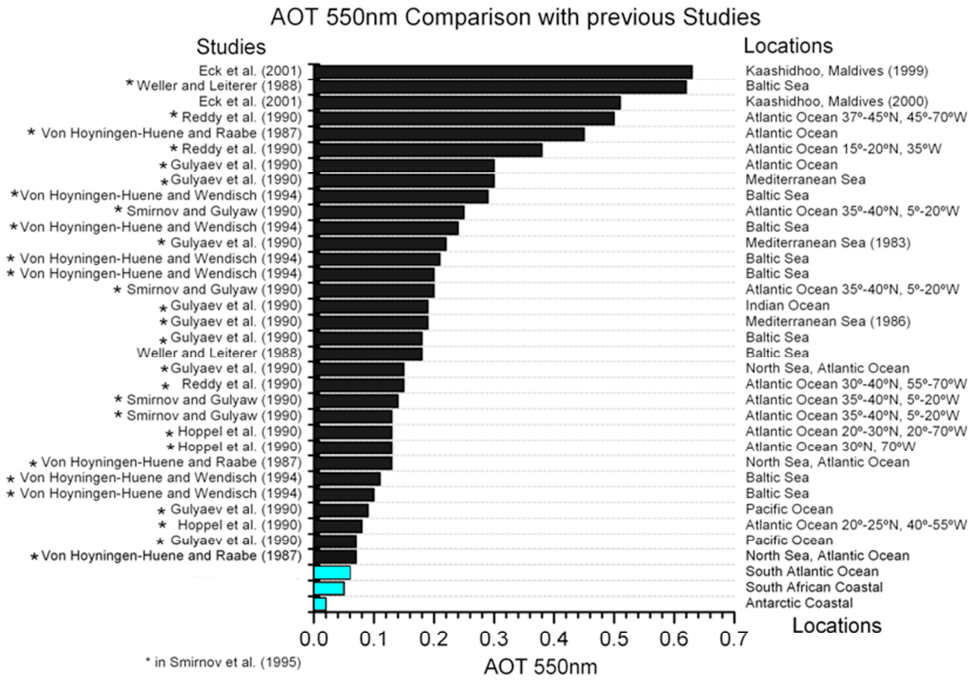

Figure 5.3. AOT 550nm comparison between this study highlighted in colour and previous research.

In conclusion, the AOT values obtained during the SANAE 47 take over cruise are consistent with prior research done on aerosol optical thickness and fall within a reasonable range. AOT is generally low with an average of between $\tau_{500nm} = 0.02 – 0.06$ describing a clean environment around the Antarctic coastal region and describing background oceanic conditions for the African coastal and Offshore region.

AERONET Comparison

Three AERONET sites situated near the study region are also analysed to compare whether the datasets show similar trends in AOT and Angstrom exponents for similar timeframes. The AERONET sites chosen as comparisons are identified as Marambio on the Antarctic Peninsula (64ºS, 56ºW), Crozet Island in the Southern Ocean (46ºS, 51ºE) and Vechernaya Hill situated in Droning Maud Land (67ºS, 46ºE). These sites are given in Figure 2.9, Chapter 2. These sites were chosen as they are the closest AERONET sites to the study area.

A comparison to AERONET (Figure 5.4) shows that the South Atlantic Ocean and Southern African Coastal have the highest AOT with an average of τ_{500nm} = 0.06 followed by Crozet Island and Marambio with an average of τ_{500nm} = 0.05. The Antarctic coastal dataset and Vechernaya Hill both experience an average AOT of τ_{500nm} = 0.03. These values correlate well with their respective locations. The South Atlantic (offshore), Southern African Coastal and Crozet Island sites describe offshore marine environments describing background oceanic conditions. The Antarctic coastal and Vechernaya Hill site correlate well describing a clean environment with some pollutants from long range transport of aerosols from marine or continental regions. Marambio does not show similar AOT but does show an average Angstrom exponent larger than 1 describing fine mode aerosols, as in the case of Antarctic Coastal and Vechernaya Hill. Both AOT and Angstrom comparisons are within a reasonable range. According to the AERONET comparison, the AOT values obtained during the SANAE 47 take over cruise are consistent with the three AERONET sites situated in and near the study area.

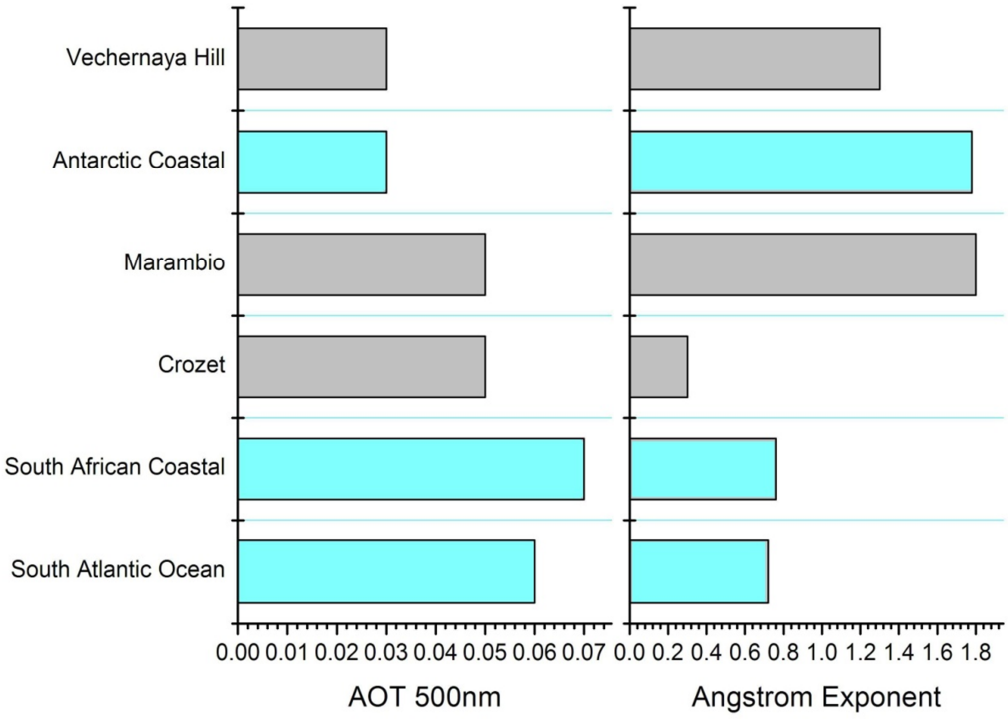

Figure 5.4. Comparison between this study shown in colour and AERONET sites.

MODIS Comparison

MODIS TERRA and AQUA aerosol product values were compared to Microtops II daily averaged AOT values for matching coordinates and days. A discrepancy was found between the MODIS TERRA and AQUA aerosol products and the Microtops II sun photometer data. Both MODIS TERRA and AQUA overestimate AOT at 550nm. Correlations between the Microtops II instrument and the MODIS TERRA aerosol product (Figure 5.5) shows an r^2 value of 0.41 and a p-value of 0.0032 while correlations to the MODIS AQUA aerosol product (Figure 5.6) shows an r^2 value of 0.49 and a p-value of 0.0024. The r^2 and p-values statistically show that MODIS significantly overestimates AOT and that the MODIS AQUA satellite is slightly more accurate than MODIS TERRA.

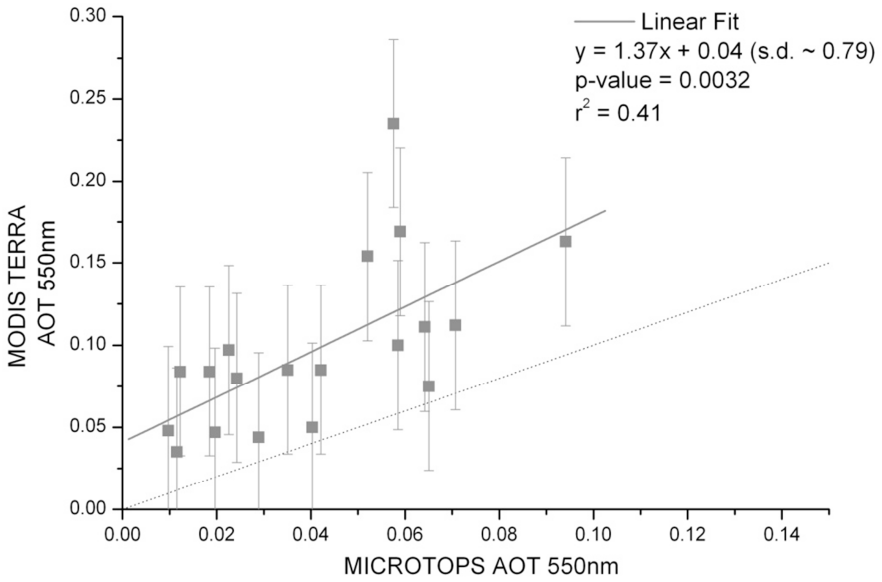

Figure 5.5. The Microtops II instrument versus the MODIS TERRA aerosol product at 550nm.

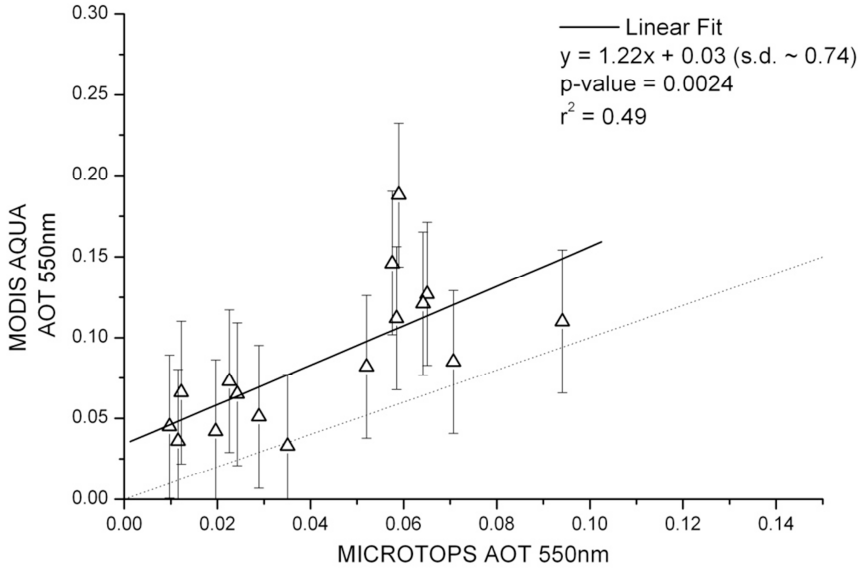

Figure 5.6. The Microtops II instrument versus the MODIS AQUA aerosol product at 550nm.

This discrepancy could be explained due to the fact that the MODIS tile size is large and averages AOT over the tile. The Microtops II takes AOT directly through the atmospheric column and would therefore be more accurate over a smaller region. It would therefore be understandable for MODIS to overestimate aerosol optical thickness over an area. Satellite AOT retrievals are most sensitive to scattering extinctions whereas sunphotometers accurately measures both the scattering and absorption (total extinction). Another factor could be the impact that sea ice and snow has on the MODIS aerosol algorithm as well as the relatively small dataset. Further inconsistencies regarding AOT values from the MODIS aerosol algorithm could be that the MODIS algorithm assumes that there is a constant wind speed of 6 meters per second, possibly lower than what is encountered. The result may cause an underestimation of ocean surface reflectance and ultimately an overestimation of AOT. Another factor could be the impact that sea ice and snow has on the MODIS aerosol algorithm as well as the relatively small dataset.

Satellite minus sun photometer retrievals were plotted as a function of the Microtops II AOT values (Figure 5.7). The graph highlights the MODIS bias towards observed low AOT values for both MODIS satellites. The findings are consistent with Smirnov et al. (2006) regarding the overestimation of satellite retrieved aerosol optical thickness measurements.

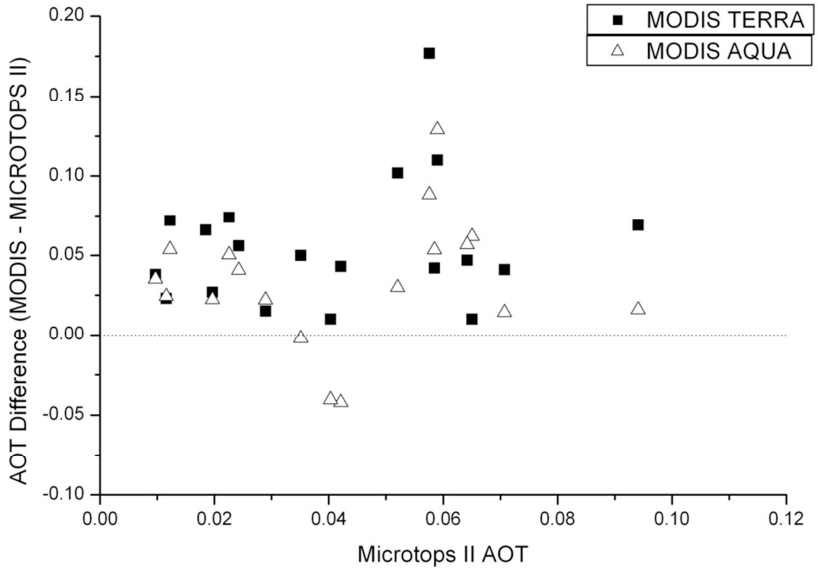

Figure 5.7. Satellite minus sunphotometer retrievals plotted as a function of Microtops II AOT values.

Chapter 6

Summary and Conclusions

A large uncertainty exists regarding aerosols and the effect they have on the earth's radiation budget and global climate change. The IPCC fourth assessment report suggests that aerosols have a net negative radiative forcing on the climate system. The distribution and concentration of aerosols is therefore of great importance regarding global warming and climate change. The purpose of this study was to present the atmospheric aerosol characteristics found over the South Atlantic, Southern Ocean and Antarctic continent as well as identify aerosol origins. A number of important findings related to aerosol optical properties, concentrations and their distribution have emerged from this study.

AOT measurements were taken during the South African National Antarctic Expedition 2007/2008 (SANAE 47) whilst onboard the M/V *S.A. Agulhas*. The voyage allowed for AOT measurements to be taken from various locations throughout the South Atlantic Ocean and Southern Ocean as well as first time AOT measurements from SANAE IV Base situated in Droning Maud land in Eastern Antarctica. The study has described the aerosol optical properties and aerosol origins for the datasets as well as made comparisons to previous AOT studies, AERONET sites and MODIS satellite. The main findings can be summarised as follows:

Aerosol Optical Properties

(1) For the entire dataset, AOT_{500nm} values showed a mean of 0.04 and a mean Angstrom value of 1.28. Statistical cluster analysis on the dataset identified two aerosol types. These aerosols types range from very fine mode to coarse mode aerosols. Aerosol types reflect those from maritime, continental and urban/industrial environments. The majority of AOT values recorded were less than 0.06.

(2) The African coastal dataset showed a mean AOT_{500nm} of 0.07 and a mean Angstrom exponent of 0.76. Cluster and statistical analyses showed two or more aerosol types evident in the dataset. Due to the location of the data points, we expect to fine aerosols from both maritime and continental environments. Fine mode aerosols experienced define similar optical properties to sulphate, nitrate and VOC aerosols. Coarse mode aerosols experienced define optical properties associated with soil dust, sea salt, biological debris and nitrate aerosols.

(3) The Offshore dataset showed a mean AOT_{500nm} of 0.06 and a mean Angstrom exponent of 0.72. Cluster and statistical analyses suggested more than one aerosol type evident in the dataset. The majority of the values identified course mode aerosols displaying similar optical properties to sea salt, biological debris and nitrate aerosols with a possibility of dust aerosols due to long range transport from continental regions. Fine mode aerosols can be attributed to sulphates, nitrates and VOC's. The optical properties describe background oceanic conditions and should contain little contamination from outside sources.

(4) The Antarctic coastal dataset showed a mean AOT_{500nm} of 0.03 and a mean Angstrom exponent of 1.78. The dataset experiences very high angstrom values and very low AOT's describing a very clean environment. Data values identify a high concentration of very fine mode aerosols describing similar optical properties to sulphates, VOC's, nitrates and ice crystal aerosols.

(5) The SANAE IV base showed a mean AOT_{500nm} of 0.02 and a mean Angstrom exponent of 2.37. These very low AOT's and high Angstrom values describe very fine mode aerosols such as sulphates, VOC's, nitrates and ice crystals. Cluster and statistical analyses suggest very few aerosol types occurring at the site and that the site is virtually unpolluted describing background atmospheric conditions for the Antarctic region.

Spatial and Temporal Characteristics

The conditions over the period December 2007 to February 2008, have given an insight into the seasonal summer aerosol conditions experienced in the study area and allowed for a baseline study into summer aerosol optical properties for the South Atlantic, Southern Ocean and Antarctica. From the study it has been possible to identify aerosol sources for the four spatial datasets chosen in the study. The 168 hour backward trajectories showed the general movement of air parcels and associated aerosols for a number of case studies and give an insight into aerosol lifetime in the atmosphere.

(6) It has been shown that there is a distinct relationship between latitude and aerosol optical properties. AOT and water vapour tend to decrease with latitude while angstrom exponent increases. Mostly course mode aerosols are identified throughout the maritime environment until roughly 65º S where the dominant aerosol type changes to fine mode. This change to predominantly fine mode aerosols occurred simultaneously with the onset of sea ice conditions.

(7) NCEP/NCAR reanalysis of surface wind vectors for the months December to February and the period 1949 – 2008 identified an as expected westerly movement of air. This westerly movement would influence the movement of aerosols from Southern Africa to the Antarctic continent as well from South America to the Southern Africa.

(8) Backward trajectories for points within the African coastal dataset showed air parcels to originate from the South American continent following the westerly winds until it reaches the Southern African coastline. Aerosols within these air parcels transported to the African coastal region would include those from maritime environments and possible long range transport of aerosols from the South American continent. Fine mode aerosols experienced are expected to originate from the South American continent while course mode aerosols are expected to originate over the South Atlantic and Southern Ocean.

(9) Backward trajectories for the offshore dataset have shown that fine mode aerosols identified in the dataset have origins over the South American continent particularly the Argentinean coastline. There is possibility of some fine mode sulphate aerosol having maritime origins. Course mode aerosols for this region have sources over the Antarctic continent and southern ocean region. We would expect the majority of course mode aerosols in this dataset to be sea salt from the surrounding marine environment.

(10) Backward trajectories for the Antarctic coastal dataset have shown that aerosols in this region have origins over the Antarctic continent and Antarctic coastal region. There are no significant aerosol sources in the region other than the maritime component. Trajectories show no long range transport of aerosols from other significant land masses.

(11) Similarly to the Antarctic coastal dataset, the SANAE IV Base shows predominantly fine mode aerosols having origins over the Antarctic continent and Antarctic coastal region. There is no long range transport of aerosols from other significant land masses only from the Southern Ocean in particular the Weddell Sea.

Comparisons

Comparisons were made between the optical properties collected in this study and previous studies regarding aerosol optical properties from various locations throughout the world. Comparison were also made between three AERONET sites situated in close proximity to the study area as well as to satellite observations regarding aerosol optical thickness (MODIS).

(12) Comparisons between this study and previous studies at 400nm, 500nm and 550nm have shown that the AOT values obtained during the voyage are consistent with previous research. Comparisons showed that the African Coastal and Offshore AOT values are similar to previous studies in those areas and that the

AOT values recorded identify background oceanic conditions. The Antarctic coastal and SANAE IV base identify very low AOT's consistent with other studies from the continent and describe a clean environment virtually free from aerosols.

(13) AOT comparisons made between this study and three AERONET sites show similar trends in AOT and Angstrom exponents. According to location, the Offshore and South African coastal sites exhibit higher AOT's than Crozet Island. The magnitude of this difference is however negligible as the standard deviation of the datasets include this difference. Measurements made in the Antarctic Coastal dataset and at Vechernaya Hill show similar AOT's and describe fine mode aerosols as the dominant aerosol type.

(14) A discrepancy between the Microtops II instrument and the MODIS TERRA and AQUA aerosol products was observed. The MODIS satellites overestimate AOT at 550nm. Reasons for this discrepancy could be the fact that MODIS averages AOT across a tile while the Microtops instrument takes a reading at a specific point through the atmospheric column. Satellite AOT retrievals are most sensitive to scattering extinctions whereas sunphotometers accurately measures both the scattering and absorption (total extinction). Another factor could be the impact that sea ice and snow has on the MODIS aerosol algorithm as well as the relatively small dataset. Further inconsistencies regarding AOT values from the MODIS aerosol algorithm could be that the MODIS algorithm assumes that there is a constant wind speed of 6 meters per second, possibly lower than what is encountered. The result may cause an underestimation of ocean surface reflectance and ultimately an overestimation of AOT. Another reason could be the impact that sea ice and snow has on the MODIS aerosol algorithm. These findings are consistent with Smirnov et al. (2006) regarding the overestimation of satellite retrieved aerosol optical thickness measurements.

ANNEX A

Definition of Statistical Parameters Used

Mean: The mathematical average of a set of numbers

Median: The middle value of an ordered set of numbers

Standard Deviation: The statistical measure of spread or variability of a set of numbers. Standard deviation is calculated as the root mean square (RMS) deviation of values from the mean.

Skewness: The degree to which a statistical distribution is not balanced around the mean. If a set of numbers has a distribution that is symmetric around the mean (Skewness of 0) then the distribution is said to be not skewed.

Kurtosis: A measure of the flatness or peakedness of a frequency distribution of numbers. Kurtosis can be platykurtic in nature (negative kurtosis) suggesting that the data values are less concentrated around the mean than the corresponding normal distribution. Kurtosis can also be leptokurtic in nature (positive kurtosis) suggesting a sharper and more acute peak around the mean suggesting a non normal distribution

ANNEX B

Definition of aerosol nature according to Angstrom Exponent

Aerosols are separated into fine mode and coarse mode aerosols according to their associated angstrom exponents. A description of fine mode and coarse mode aerosols types is given:

- Fine mode aerosols are classified as those particles having an Angström exponent of greater than 1. Fine mode aerosols include the following aerosols: sulphates from biogenic gas such as DMS and SO_2, nitrates from NO_x and organic matter from VOC's. These types of aerosols are located in and around continental regions and include both natural and anthropogenic aerosols (Seinfeld and Pandis, 1998). In the Antarctic environment Six et al. (2005) suggest that sulphates, VOC's, nitrates and diamond dust events (ice crystals) comprise the majority of the fine mode aerosols experienced.

- Coarse mode aerosols are classified as those particles having an Angström exponent of less than 1. Coarse mode aerosols identified could include the following aerosols: soil dust, sea salt, biological debris and Nitrates from NO_x (Seinfeld and Pandis, 1998).

References

AERONET, 2008, *Maritime Aerosol Network*
<http://aeronet.gsfc.nasa.gov/new_web/maritime_aerosol_network.html>
(25 April 2008)

Charlson, R.J., Schwartz, S.E., Hales, J.M., Cess, R.D., Coakley, J.A., Jnr, Hansen, J.E. and Hofmann, D.J. 1992: Climate Forcing by anthropogenic aerosols, *Science*, **255**, 423-430.

Cobourn, W.G, and Hubbard, M.C. 1999: An enhanced ozone forecasting model using air mass trajectory analysis, *Atmospheric Environment,* **33,** 4663 – 4674.

Dubovik, O., Holben, B., Eck, T.F., Smirnov, A., Kaufman, Y.J., King, M.D., Tanré, D., and Slutsker, I., 2001: Variability of Absorption and Optical Properties of Key Aerosol Types Observed in Worldwide Locations, *Journal of the Atmospheric Sciences, **59,** 590 – 608.*

Dubovik, O., King, M.D., 2000: A Flexible Inversion Algorithm for Retrieval of Aerosol Optical Properties from Sun and Sky Radiance Measurements, *Journal of Geophysical Research,* **105**, D16, 20,673 – 20,696.

Eck, T.F., Holben, B.N., Dubovik, O., Smirnov, A., Goloub, P., Chen, H.B., Chatanet, B., Gomes, L., Zhang, X.Y., Tsay, S.C., Ji, Q., Giles D., and Slutsker, I., 2005: Columnar aerosol optical properties at AERONET sites in central eastern Asia and aerosol transport to the tropical mid-Pacific, *Journal of Geophysical Research,* **110,** D06202, doi:10.1029/2004JD005274.

Eck, T.F., Holben, B.N., Dubovik, O., Smirnov, A., Slutsker, I., Lober, M., and Ramathan, V., 2001: Column-integrated aerosol optical properties over the Maldives

during the northeast monsoon for 1998–2000, *Journal of Geophysical Research*, 106, D22, 28,555–28,566,

Forster, P., V. Ramaswamy, P. Artaxo, T. Berntsen, R. Betts, D.W. Fahey, J. Haywood, J. Lean, D.C. Lowe, G. Myhre, J. Nganga, R. Prinn, G. Raga, M. Schulz and R. Van Dorland, 2007: Changes in Atmospheric Constituents and in Radiative Forcing. *In: Climate Change 2007: The Physical Science Basis. Contribution of Working Group I to the Fourth Assessment Report of the Intergovernmental Panel on Climate Change* [Solomon, S., D. Qin, M. Manning, Z. Chen, M. Marquis, K.B. Averyt, M. Tignor and H.L. Miller (eds.)]. Cambridge University Press, Cambridge, United Kingdom and New York, NY, USA.

Gadhavi, H., and Jayaraman, A., 2004: Aerosol characteristics and aerosol radiative forcing over Maitri, Antarctica, *Current Science,* **86,** 2, 296 – 304.

Gobbi, G.P., Kaufman, Y.J., Koren, I., and Eck, T.F., 2007: Classification of aerosol properties derived from AERONET direct sun data, *Atmospheric Chemistry and Physics, 7,* 453 – 458.

Haywood, J., Francis, P., Dubovik, O., Glew, M., and Holben, B., 2003: Comparison of aerosol size distributions, radiative properties, and optical depths determined by aircraft observations and Sun photometers during SAFARI 2000, *Journal of Geophysical Research,* **105**, D13, 8471.

Haywood, J.M. and Boucher, O., 2000: Estimates of the direct and indirect radiative forcing due to tropospheric aerosols: A review, *Review of Geophysics,* **38**, 513 – 543.

Hobbs, P.V, 2000: *Introduction to Atmospheric Chemistry*, Cambridge University Press, United States of America, 82-110.

Ichoku, C., Levy, R., Kaufman, Y.J., Remer, L.A., Li, R., Martins, V.J., Holben, B.N., Abuhassan, N., Slutsker, I., Eck, T.F., and Pietras, C., 2002: Analysis of the

performance characteristics of the five-channel Microtops II Sun photometer for measuring aerosol optical thickness and precipitable water vapour, *Journal of Geophysical Research,* **17,** D13, doi: 10.1029/2001JD001302.

IPCC Report, 2007: *Climate Change 2007: The Physical Science Basis. Contribution of Working Group I to the Fourth Assessment Report of the Intergovernmental Panel on Climate Change*, S. Solomon, D. Qin, M. Manning, Z. Chen, M. Marquis, K.B. Averyt, M. Tignor, and H.L. Miller (eds.), Cambridge University Press, Cambridge, United Kingdom and New York, NY, 996 pp.

Jacob, D.J, Andreae, M.O., Bigg, E.K., Duce, R.A., Fung, I., Hidy, G.M., Legrand, M., Prospero, J.M., Raes, F., Warren, S.G., and Wiedensohler, A., 1995: *Group Report: What Factors Influence Atmospheric Aerosols, How Have They Changed in the Past, and How Might They Change in the Future,* in Aerosol Forcing of Climate Edited by R.J. Charlson and J. Heintzenburg, John Wiley & Sons, 183 – 195.

Kalnay, E., M. Kanamitsu, R. Kistler, W. Collins, D. Deaven, L. Gandin, M. Iredell, S. Saha, G. White, J. Woollen, Y. Zhu, M. Chelliah, W. Ebisuzaki, W. Higgins, J. Janowiak, K.C. Mo, C. Ropelewski, J. Wang, A. Leetmaa, R. Reynolds, R. Jenne, and D. Joseph, 1996: The NCEP/NCAR 40-Year Reanalysis Project., *Bull. Amer. Meteor. Soc.*, 77, **3**, 437-470.

Kay, M.J., and Box, M., 2000: Radiative effects of absorbing aerosols and the impact of water vapor, *Journal of Geophysical Research, **105**,* 12,221 – 12,234.

Keil, A. and Haywood, J.M., 2003: Solar radiative forcing biomass burning aerosol particles during SAFARI 2000: A case study based on measured aerosol and cloud properties, *Journal of Geophysical Research*, **108**, D13, 8467, doi: 10.1029/2002JD002315, SAF 3:1-10.

King, M.D., Byrne, D.M., Herman, B.M., and Reagan, J.A., 1978: Aerosol Size Distributions Obtained by Inversion of Spectral Optical Depth Measurements, *Journal of the Atmospheric Sciences,* **35,** 2153 – 2167.

Knobelspiesse, K.D., Pietras, C., Fargion, G.S., Wang, M., Frouin, R., Miller, M.A., Subramaniam, A., and Balch, W.M., 2004: Maritime aerosol optical thickness measured by handheld sun photometers*, Remote Sensing of Environment*, **93**, 87 – 106.

Liley, J.B., and Forgan, B.W., 2009: Aerosol optical depth over Lauder, New Zealand, *Geophysical Research Letters,* **36,** L07811.

Masmoudi, M., Chaabane, M., Tanré, D., Gouloup, P., Blarel, L., and Elleuch, F., 2003: Spatial and temporal variability of aerosol: size distribution and optical properties, *Atmospheric Research,* **66,** 1 – 19.

Morys, M., Mims III, F.M., and Anderson, S.E., 2003: In User's Guide: Chapter 9: *Theory of operation: Design, calibration and performance of Microtops II hand-held ozonometer,* Solar Light Company Inc. United States of America.

O'Dowd, C., Smith, M.H., Consterdine, I.E., and Lowe, J.A., 1997: Marine Aerosol, Sea-Salt, and the Marine Sulphur Cycle: A Short Review, *Atmospheric Environment,* **31**, 73 – 80.

Peixoto, J.P., and Oort, A.H., 1992: *Physics of Climate,* American Institute of Physics, Unites States of America.

Porter, J.N., Miller, M., Pietras, C., and Motell, C., 2000: Ship-Based Sun Photometer Measurements Using Sun Photometers, *Journal of Atmospheric and Oceanic Technology, **18,*** 765 – 774.

Power, H.C., 2003: The geography and climatology of aerosols, *Progress in Physical Geography,* **27**, 4, 502–547.

Redemann, J., Turco, R.P., Liou, K.N., Russel, P.B., Bergstrom, R.W., Schmid, B., Livingston, J.M., Hobbs, P.V., Hartley, W.S., Ismail, S., Ferrare, R.A., and Browell, E.V., 2000: Retrieving the vertical structure of the effective aerosol complex index of refraction from a combination of aerosol in situ and remote sensing measurements during TARFOX, *Journal of Geophysical Research,* **105**, 8, 9949 – 9970.

Ritter, M. E., 2006: *The Physical Environment: an Introduction to Physical Geography*. <http://www.uwsp.edu/geo/faculty/ritter/geog101/textbook/title_page.html>
(30 May 2008)

Queface, A.J., Piketh, S.J., Annegarn, H.J., Holben, B.N. and Uthui, R.J, 2003: Retrieval of aerosol optical thickness and size distribution from the CIMEL Sun photometer over Inhaca Island, Mozambique, *Journal of Geophysical Research,* **108(D13),** 8509, doi:10.1029/2002JD002374.

Sakerin, S.M., Smirnov, A., Kabanov, D.M., Pol'kin, V.V., Panchenko, M.V., Holben, B.N., and Kopelevich, O.V., 2007: Aerosol optical and microphysical properties over the Atlantic Ocean during the 19th cruise of the Research Vessel *Akademik Sergey Vavilov*, *Journal of Geophysical Research*, **112**, 1 – 9, doi:10.1029/2006JD007947.

Seinfeld, J.H., and Pandis, S.N., 1998: *Atmospheric Chemistry and Physics – From Air Pollution to Climate Change,* John Wiley & Sons Inc., Canada.

Six, D., Fily, M., Blarel, L., Goloub, P., 2005: First aerosol optical thickness measurements at Dome C (East Antarctica), summer season 2003 – 2004, *Atmospheric Environment,* **39**, 5041 – 5050.

Smirnov, A., Villevalde, Y., O'Neill, N.T, Royer, A., and Tarussov, A., 1995: Aerosol optical depth over the oceans: Analysis in terms of synoptic air mass types, *Journal of Geophysical Research,* **100**, NO. D8, 16,639-16,650.

Smirnov, A., Holben, B.N., Eck, T.F., Dubovik, O., and Slutsker, I., 2000: Cloud-Screening and Quality Control Algorithms for the AERONET Database, *Remote Sensing of Environment,* **73**, 33 –349.

Smirnov, A., Holben, B.N., Dubovik, O., O'Neill, N.T., Eck, T.F., Westphal, D.G., Goroch, A.K., Pietras, C., and Slutsker, I., 2002a: Atmospheric Aerosol Optical Properties in the Persian Gulf, *Journal of the Atmospheric Sciences,* **59**, 620 – 634.

Smirnov, A., Holben, B.N., Kaufman, K.J., Dubovik, O., Eck, T.F., Slutsker, I., Pietras, C., and Halthore, R.N., 2002b: Optical Properties of Atmospheric Aerosol in Maritime Environments, *Journal of the Atmospheric Sciences,* **59,** 501 – 523.

Smirnov, A., B. N. Holben, O. Dubovik, R. Frouin, T. F. Eck, and I. Slutsker, 2003: Maritime component in aerosol optical models derived from Aerosol Robotic Network data, Journal of Geophysical Research, **108(D1)**, 4033, doi:10.1029/2002JD002701.

Smirnov, A., Holben, B.N., Sakerin, S.M., Kabanov, D.M., Slutsker, I., Chin, M., Diehl, T.M., Remer, A., Kahn, R., Ignatov, A., Liu, L., Mishchenko, M., Eck, T.F., T. L. Kucsera, D. Giles, and O. V. Kopelevich, 2006: Ship-based aerosol optical depth measurements in the Atlantic Ocean: Comparison with satellite retrievals and GOCART model, *Geophysical Research Letters, **33,*** L14817, 1 – 4.

Smirnov, A., Holben, B.N., Slutsker I., Giles D.M., McClain C.R., Eck, T.F., Sakerin, S.M., Macke, A., Croot, P., Zibordi, G., Quinn, P.K., Sciare, J., Kinne, S., Harvey, M., Smyth, T.J., Piketh, S., Zielinski, T., Proshutinsky, A., Goes, J.I., Nelson, N.B., Larouche, P., Radionov, V.F., Goloub, P., Krishna Moorthy, K., Matarrese, R.,

Robertson, E.J., and Jourdin, F., 2009: Maritime Aerosol Network as a component of Aerosol Robotic Network, *Journal of Geophysical Research,* **114**, 1 – 10, doi:10.1029/2008JD011257.

Solar Light Company, 2003, *User's guide, Microtops II, Sunphotometer Version 5.5*, Solar Light Company Inc, United Stated of America.

Solomon, S., D. Qin, M. Manning, R.B. Alley, T. Berntsen, N.L. Bindoff, Z. Chen, A. Chidthaisong, J.M. Gregory, G.C. Hegerl, M. Heimann, B. Hewitson, B.J. Hoskins, F. Joos, J. Jouzel, V. Kattsov, U. Lohmann, T. Matsuno, M. Molina, N. Nicholls, J. Overpeck, G. Raga, V. Ramaswamy, J. Ren, M. Rusticucci, R. Somerville, T.F. Stocker, P. Whetton, R.A. Wood and D. Wratt, 2007: Technical Summary. In: *Climate Change 2007: The Physical Science Basis. Contribution of Working Group I to the Fourth Assessment Report of the Intergovernmental Panel on Climate Change* [Solomon, S., D. Qin, M. Manning, Z. Chen, M. Marquis, K.B. Averyt, M. Tignor and H.L. Miller (eds.)]. Cambridge University Press, Cambridge, United Kingdom and New York, NY, USA.

Swart, S., Ansorge, I., Swart, N., Rae, K., Burls, N., and Funke, M., 2006: Good Hope V: Hydrographic, Biological and Meteorological Cruise Report, *UCT Oceanographic Report 06-1*, University of Cape Town.

Tyson, P.D., Preston-Whyte, R.A., 2000: *The Weather and Climate of Southern Africa,* Oxford University Press, South Africa.

Vinoj, V., Anjan, A., Sudhakar, M., Satheesh, S.K., Srinivasa, J., and Moorthy, K.K., 2007: Latitudinal variation of aerosol optical depths from northern Arabian Sea to Antarctica, *Geophysical Research Letters,* **34**, 1 – 5, doi:10.1029/2007GL029419.

Walden, V.P., Warren, S.G., and Tuttle, E., 2003: Atmospheric Ice Crystals over the Antarctic Plateau in Winter, *American Meteorological Society,* **42,** 1391 – 1405.

Wyputta, U., 1997: On the transport of trace elements into Antarctica using measurements at the Georg-von-Neumayer station, *Tellus*, **49B,** 93 – 111.